Design, Synthesis, and Biological Evaluation of Monopyrrolinone-Based HIV-1 Protease Inhibitors

Amos B. Smith, III,*,† Louis-David Cantin,† Alexander Pasternak,† Lisa Guise-Zawacki,† Wenquin Yao,† Adam K. Charnley,† Joseph Barbosa,† Paul A. Sprengeler,† Ralph Hirschmann,† Sanjeev Munshi,‡ David B. Olsen,‡ William A. Schleif,‡ and Lawrence C. Kuo‡

Department of Chemistry, University of Pennsylvania, 231 South 34th Street, Philadelphia, Pennsylvania 19104, and Merck Research Laboratories, West Point, Pennsylvania 19486

Received October 17, 2002

The design, synthesis, and biological evaluation of a series of HIV-1 protease inhibitors [(−)-**6**, (−)-**7**, (−)-**23**, (+)-**24**] based upon the 3,5,5-trisubstituted pyrrolin-4-one scaffold is described. Use of a monopyrrolinone scaffold leads to inhibitors with improved cellular transport properties relative to the earlier inhibitors based on bispyrrolinones and their peptide counterparts. The most potent inhibitor (−)-**7** displayed 13% oral bioavailability in dogs. X-ray structure analysis of the monopyrrolinone compounds cocrystallized with the wild-type HIV-1 protease provided valuable information on the interactions between the inhibitors and the HIV-1 enzyme. In each case, the inhibitors assumed similar orientations for the P2′-P1 substituents, along with an unexpected hydrogen bond of the pyrrolinone NH with Asp225. Interactions with the S2 pocket, however, were not optimal, as illustrated by the inclusion of a water molecule in two of the three inhibitor−enzyme complexes. Efforts to increase affinity by displacing the water molecule with second and third generation inhibitors did not prove successful. Lack of success with this venture is a testament to the difficulty of accurately predicting the many variables that influence and build binding affinity. Comparison of the inhibitor positions in three complexes with that of Indinavir revealed displacements of the protease backbones in the enzyme flap region, accompanied by variations in hydrogen bonding to accommodate the monopyrrolinone ring. The binding orientation of the pyrrolinone-based inhibitors may explain their sustained efficacy against mutant strains of the HIV-1 protease enzyme as compared to Indinavir.

Introduction

The human immunodeficiency virus (HIV) encodes four enzymes, which comprise potential targets for therapeutic intervention.[1] Reverse transcriptase inhibitors, typified by AZT, provided the first approved anti-HIV drug.[2] Approval of peptidal inhibitors of the viral protease, including Amprenavir, Indinavir, Lopinavir, Nelfinavir, Ritonavir, and Saquinavir, which converts the Gag−Pol fusion polyprotein into the active constituents,[3] has proven invaluable as an addition to the armamentarium of the physician.[4] Moreover, administration of a cocktail of anti-acquired immunodeficiency syndrome (AIDS) drugs, including nucleoside and/or nonnucleoside reverse transcriptase inhibitors, combined with protease inhibitors, allows both the prevention of viral replication and the development of resistance[5] at low, less toxic doses of the components[6] but does not eradicate the latent virus.[7] Thus, development of drug resistance remains a serious concern in anti-AIDS therapy. It is possible, however, that HIV protease inhibitors in which the conventional peptide backbone has been replaced, as in the case with Tipranavir,[8] the cyclic ureas,[9] and the pyrrolinones,[10] will bind differently from the approved peptidal inhibitors and thereby reduce the ability of the virus to generate resistant mutations.[11]

A major thrust of our efforts in the field of nonpeptide peptidomimetics during the past 10 years has been the development of the pyrrolinone scaffold, which depending on the precise structure can effectively mimic the β-strand/β-sheet and/or turn conformations of peptides, both in solution and in the solid state.[12] The early ability of the polypyrrolinones to mimic peptide extended conformations prompted us to explore the use of this scaffold for the generation of aspartic acid and related protease inhibitors.[10] At the outset of this effort, we reasoned that the pyrrolinone scaffold would have increased hydrolytic stability due to the lack of the peptide bonds.[10] This hypothesis has proven valid; to date, we have designed and synthesized successful inhibitors of renin,[13] the HIV-1 protease,[14] and matrix metalloproteases.[15] In addition, we recently disclosed a high affinity peptide−pyrrolinone hybrid ligand for the class II major histocompatibility complex (MHC) protein HLA-DR1, which was shown by X-ray analysis to bind with remarkable similarity to the native peptide.[16]

Our early work on HIV-1 protease inhibitors led to bispyrrolinones (−)-**1** and (−)-**2** (Figure 1), which displayed nanomolar activity (ca. IC_{50} of 10 and 1.3 nM, respectively).[14b] Moreover, these inhibitors displayed improved CIC_{95}/IC_{50} ratios[17] relative to their peptidal counterpart **3**, suggestive of improved cellular membrane permeability.

We proposed that the improved CIC_{95}/IC_{50} ratios were due to the intramolecular hydrogen bonding between the two pyrrolinone rings.[18] Unfortunately, our most

* To whom correspondence should be addressed. Tel: 215-898-4860. Fax: 215-898-5129. E-mail: smithab@sas.upenn.edu.
† University of Pennsylvania.
‡ Merck Research Laboratories.

10.1021/jm0204587 CCC: $25.00
Published on Web 04/09/2003

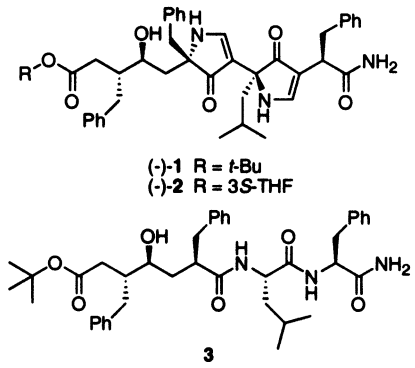

Figure 1.

potent inhibitor, (−)-**2**, displayed no oral bioavailibility in dogs. We suspected that the lack of oral bioavailability was due at least in part to the relatively high molecular weight (ca. >730). We were however encouraged by the potency of the bispyrrolinone inhibitors. To improve these inhibitors, we explored the use of the monopyrrolinone scaffold. Herein, we report on the design, synthesis, and biological evaluation of three monopyrrolinone-based inhibitors, including X-ray analysis of the three inhibitors cocrystallized with the wild-type HIV-1 protease.

Initial Design of a Monopyrrolinone HIV-1 Protease Inhibitor. In an effort to reduce the molecular weight of (−)-**1** and (−)-**2** (Figure 1) while retaining the important points of contact with the enzyme, we were drawn to peptidal inhibitors **4** and **5** (Figure 2) as lead structures for the design of monopyrrolinone-based inhibitors.[14a,19] These peptidal inhibitors had proven highly potent in isolated enzyme assays, and **5** displayed excellent antiviral activity, albeit with poor bioavailability due, we believe, to the peptidal nature of the structure. We envisioned that replacement of the amide functionality in **4** and **5** with a monopyrrolinone scaffold would not only lead to prospective HIV-1 protease inhibitors with reduced molecular weights as compared to (−)-**1** and (−)-**2** but, in turn, to inhibitors with improved bioavailability.

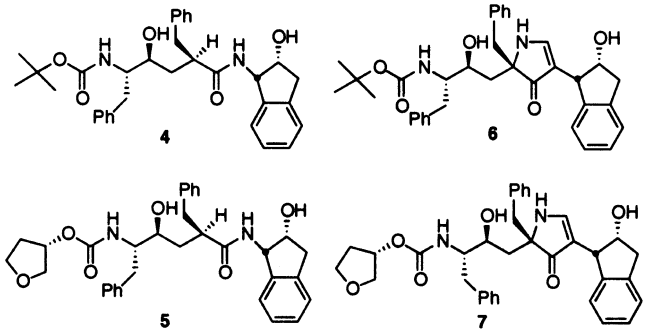

Figure 2.

To determine whether the simplified scaffold would maintain the proper binding orientation of the side chains (P1, P1′, P2, P2′) in the HIV-1 protease, we carried out a series of molecular modeling studies. Installation of the appropriate side chains on the monopyrrolinone scaffold led to **6** and **7** (Figure 2), possessing molecular weights of 568 and 582, respectively. Monte Carlo conformational searches, with both the chloroform and the water continuum solvation models, revealed good overlay between the lowest energy conformers of **6** and **7** and the reported structures of the peptidal inhibitors MVT-101 (AcHN-Thr-Ile-Nle-Nle-Gln-Arg-C(O)NH_2)[20] and JG-365 (AcHN-Ser-Leu-Ans-Phe-ψ[CH(OH)CH_2N]-Pro-Ile-Val-OMe)[20] cocrystallized with the wild-type HIV-1 protease. To determine if the pyrrolinone NH in **6** and **7** was positioned appropriately to participate in hydrogen bonding with the enzyme, the lower energy conformations of **6** and **7** and their peptidal counterparts (**4** and **5**) were energy-minimized in the active site of HIV-1 protease, using the MM2X force field, according to the published protocols of Holloway et al.[21] Both **6** and **7** displayed similar conformations to each other and to their peptidal counterparts. Notably, **6** and **7** appeared to generate the required hydrophobic interactions with the active site of the enzyme, along with the requisite hydrogen-bonding interactions between both the transition state mimic hydroxyl and the catalytic diad (Asp25/Asp225) and the carbamate, the pyrrolinone carbonyls, and the well-known flap water.[20]

Further analysis of the modeled complexes revealed that removal of the amide from the backbone to form the pyrrolinone ring led to a conformation that precluded formation of a hydrogen bond between the pyrrolinone NH with Gly27. A second potential disadvantage of the monopyrrolinone design was the lack of possible intramolecular hydrogen bonding as observed when two pyrrolinone rings are linked (Figure 3). We suggested that this intramolecular hydrogen bonding, in conjunction with the steric effects of the side chains, is responsible for the extended β-strand/β-sheet arrangement of polypyrrolinones[22] and may also contribute significantly to the improved antiviral activity observed for (−)-**1** and (−)-**2** over their amide counterparts.[14b] We also reasoned that the effects of losing the interring pyrrolinone hydrogen bond may be mitigated by formation of an intramolecular hydrogen bond between the pyrrolinone NH and the adjacent secondary hydroxyl group (**II**, Figure 3).

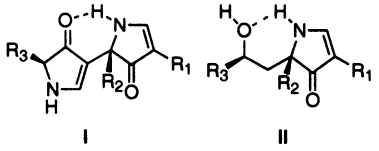

Figure 3.

Synthesis of Prospective Inhibitors 6 and 7. Confident in the new design, we embarked on the synthesis of **6** and **7**, envisioned to take advantage of our now general pyrrolinone synthetic protocol,[14b] which called for condensation of the known amino-ester (+)-**8**[14b] with aldehyde **9**, followed by metalloenamine-mediated pyrrolinone ring formation (Scheme 1).

Two approaches for the construction of **9** were explored. The first began with known cyclobutanone **10**[23] (Scheme 2, route A). Addition of the lithium anion derived from sulfoximine (−)-**11**, according to the resolution method of Johnson,[24] provided a mixture of diastereomers from which (−)-**12** could be separated with some difficulty by fractional recrystallization. The absolute stereochemistry of (−)-**12** was determined by single-crystal X-ray analysis. Thermolysis then provided cyclobutanone (−)-**13** along with recovery of sulfoximine

Scheme 1

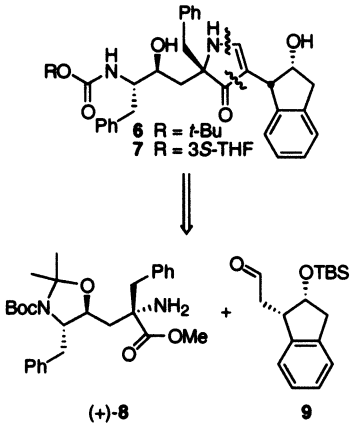

(−)-**11**. Lactone (−)-**14** was then generated by Baeyer−Villiger oxidation of (−)-**13** (ca. 90% yield).[25] Alternatively, racemic lactone **14**[23a] could be resolved via condensation with L-phenethylamine, utilizing the Weinreb protocol[26] (Scheme 2, route B). The resultant diastereomers (−)-**15** and (−)-**16** were separated by column chromatography; the absolute stereochemistry of (−)-**15** was again ascertained by single-crystal X-ray analysis. Subsequent exposure of (−)-**15** to p-TSA afforded the desired lactone (−)-**14**. Although the two routes proceeded with comparable yields and number of steps, the easier separation of (−)-**15** and (−)-**16** facilitated the generation of enantiomerically pure (−)-**14** in a more efficient manner.

Scheme 2

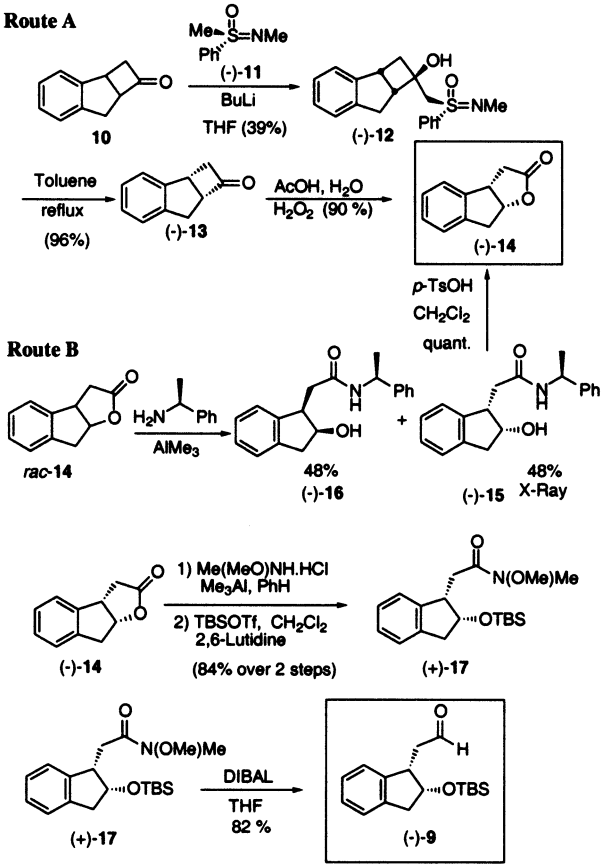

With ample quantities of (−)-**14** in hand, aldehyde (−)-**9** was then prepared in three steps by conversion to the corresponding Weinreb amide, protection of the secondary hydroxyl as a TBS ether, and reduction with DIBAL.

Pyrrolinone ring construction was next achieved by condensation of aldehyde (−)-**9** with amino-ester (+)-**8**, followed in turn by metalation of the intermediate imine with KHMDS, and intramolecular addition of the metalloimine to the ester carbonyl (Scheme 3). Removal of the protective groups under acidic conditions (1 N HCl/MeOH) then afforded (+)-**19**, which served as precursor to both targets (−)-**6** and (−)-**7** as outlined in Scheme 3.[27]

Scheme 3

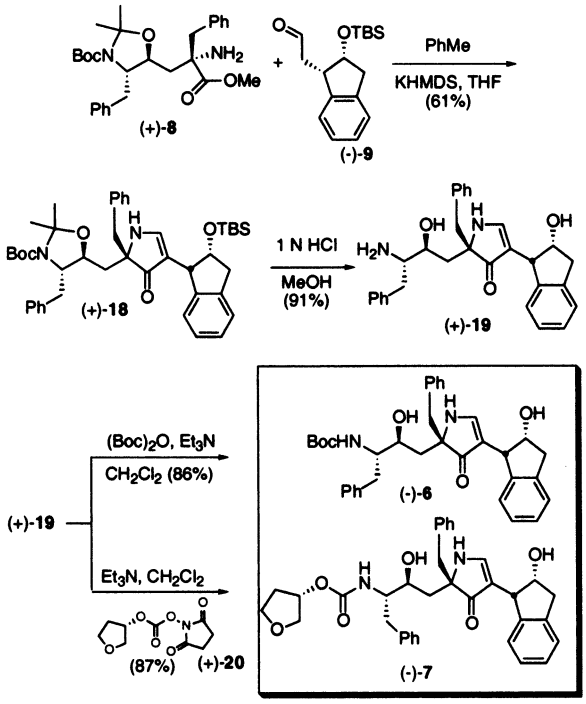

Biological Evaluation of (−)-6 and (−)-7. Purified enzyme assays[28] of (−)-**6** and (−)-**7** revealed that the tetrahydrofuran (THF) carbamate congener [(−)-**7**, 2.0 nM], as observed in the bispyrrolinone series, displays a modest increase in binding affinity as compared to the *tert*-butyl carbamate [(−)-**6**, 11.0 nM]. However, when compared to the potencies of their amide counterparts (**4** and **5**), the monopyrrolinone inhibitors were less active, in both the isolated enzyme and the cellular assays[29] (Table 1). The ratio of the cellular antiviral activity over the isolated enzyme potency (CIC_{95}/IC_{50} ratio), however, was comparable to that of Indinavir. We take the CIC_{95}/IC_{50} ratio as an indication of the ease

Table 1. Bioassay Data for Pyrrolinone Inhibitors and Related Amide-Based Inhibitors

inhibitor	IC_{50} (nM)	CIC_{95} (nM)	C/I
(−)-**1**	10	1500	150
(−)-**2**	1.3	800	615
3	0.6	6 000	10 000
4	0.3	400	1333
5	0.03	3	100
(−)-**6**	11.9	800	67
(−)-**7**	2.0	100−250	50−125
(−)-**23**	2.0	250	125
(+)-**24**	5.7	781	137
Indinavir	0.36	25−100	69−277

of transport across the cellular membrane.[18] Thus, it would appear that the monopyrrolinone inhibitors have improved cell membrane transport properties as compared both to their amide counterparts **4** and **5** and to the previously designed bispyrrolinones (−)-**1** and (−)-**2**.

We next determined the oral bioavailability of our best monopyrrolinone inhibitor (−)-**7**. Administration of (−)-**7** in two dogs revealed an oral bioavailability of 13%, with a $t_{1/2}$ of 33−36 min, a clearance rate of 20.6 mL/min/kg, a volume distribution of 0.81 L/kg, and an area under the curve of 1.83×10^6 μM/h.[14,29] Unfortunately, the corresponding data for amide **5** do not exist. Taken together, the results from the purified enzyme assays and oral bioavailability studies validate our design premise that use of the monopyrrolinone scaffold as a mimic of a segment of a peptide backbone can lead to viable HIV-1 protease inhibitors with improved oral bioavailability vis à vis the bispyrrolinones.

X-ray Crystal Analysis: The Structure of Pyrrolinone (−)-7 Cocrystallized with Wild-Type HIV-1 Protease. To understand the interactions of the monopyrrolinone scaffold with the protease and possibly to explain the loss of affinity of (−)-**7** as compared to **5**, the structure of (−)-**7** bound to wild-type HIV-1 protease was elucidated via X-ray crystallographic analysis (Figure 4).[30,31] As the earlier molecular modeling studies

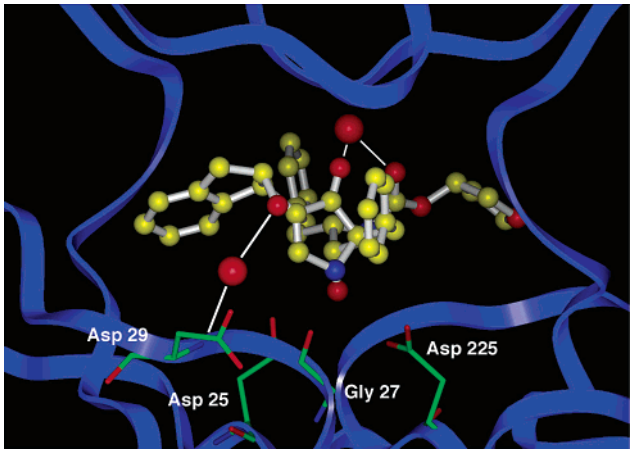

Figure 4. Structure of (−)-**7** cocrystallized with wild-type HIV-1 protease.

had predicted, the relatively large distance between the pyrrolinone NH and the Gly27 did indeed prevent hydrogen bond formation. The system, however, compensates for this energetic loss by formation of a hydrogen bond between the pyrrolinone NH and the enzyme Asp225 carboxylate, a process that requires a 50° rotation of the Asp225 carboxylate relative to the orientation observed in the Indinavir−HIV-1 protease complex.[32] Further comparison of the crystal structures of enzyme-bound (−)-**7** and Indinavir (Figure 4) revealed shifts of the protease backbone in both the flap and the Thr26-Asp30 regions to accommodate the pyrrolinone ring. The resultant larger than expected space (5.4 Å) between the Indane hydroxyl in (−)-**7** and the enzyme Asp29 NH permits incorporation of a hydrogen-bound water molecule. Similar bound water molecules in HIV-1 proteases have been observed in both the presence and the absence of an inhibitor.[33]

Design, Synthesis, and Biological Evaluation of Second Generation Monopyrrolinone-Based HIV-1 Protease Inhibitors. To increase the binding affinity of an enzyme inhibitor, the numerous thermodynamic parameters that affect binding affinity must be addressed.[34] Unfortunately, prediction of the entropic energy gain upon displacement of a water molecule from the active site of the enzyme−inhibitor complex is difficult.[35a,36] As a result, rational attempts to increase affinity have met with both success[24] and failure.[37] Despite these challenges, we undertook the design and synthesis of a series of second generation monopyrrolinone-based inhibitors possessing P2 side chains chosen to displace the active site water molecule, with the expectation of enhancing the inhibitor binding affinity. Toward this end, molecular modeling, employing the X-ray structure of (−)-**7** bound to the HIV-1 protease, led to the design of **23** (Scheme 4), possessing a carbamate moiety at P2, which we envisioned would displace the water molecule and thereby reestablish a hydrogen bond between the inhibitor and the Asp29 in the protease.

Scheme 4

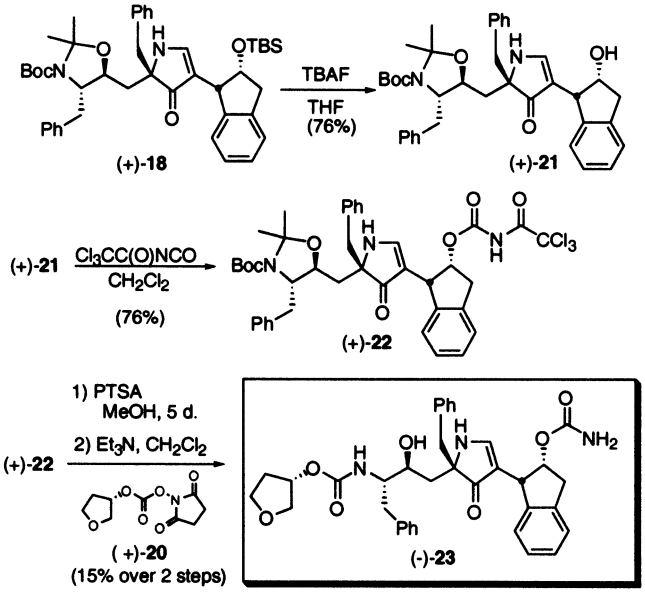

Initial attempts to convert (−)-**7** directly to **23** via treatment with trichloroacetyl isocyanate[38] failed due to the lack of chemoselectivity between the two secondary hydroxyls. The synthesis of **23** was however achieved, beginning with (+)-**18** prepared previously. Removal of the TBS protecting group with TBAF permitted selective introduction of the trichloroacetyl-protected carbamate moiety[38] to furnish (+)-**22** (Scheme 4). Prolonged treatment of (+)-**22** with *p*-toluenesulfonic acid in MeOH (ca. 5 days) eventually effected removal of the remaining protecting groups. Exposure to (+)-**20**[27] completed construction of (−)-**23**.

In the purified enzyme and cellular assays, (−)-**23** displayed similar binding affinity (ca. 2.0 nM against wild-type HIV-1) to that observed for (−)-**7** (Table 1). Importantly, the X-ray crystal structure of (−)-**23** bound to wild-type HIV-1 protease revealed that the water molecule had indeed been displaced from the active site (Figure 5).[39] However, the hydrogen-bonding angles

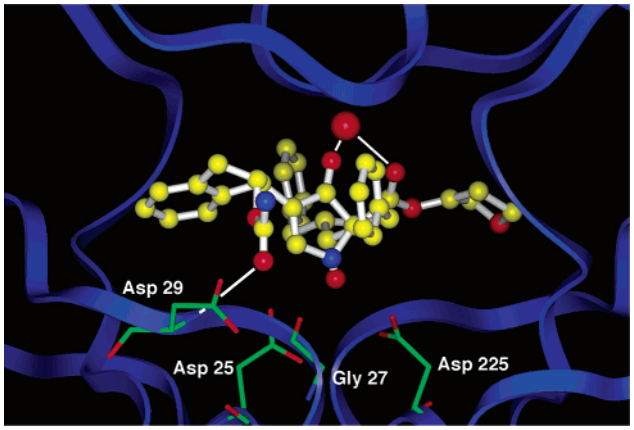

Figure 5. Structure of (−)-**23** cocrystallized with wild-type HIV-1 protease.

observed between the carbonyl of the carbamate and the NH of Asp29 proved nonoptimal (∠NHO 152°, ∠COH 113°, 2.36 Å). Possibly, the resultant weakened hydrogen bond in the enzyme−inhibitor complex, when combined with the entropic cost of rigidifying the free-rotating carbamate, is sufficient to override the entropic gain obtained by removing the water molecule from the active site and thereby leads to no improvement in potency.

To address the binding affinity issue, we attempted to optimize the orientation of the P2 side chain. Further molecular modeling suggested congener **24** (Scheme 5), possessing a tetrahydroisoquinolyl P2 side chain. In addition to displaying good hydrogen-bonding characteristics in the modeling studies, we anticipated that preorganization of the side chain would further enhance binding affinity.

Scheme 5

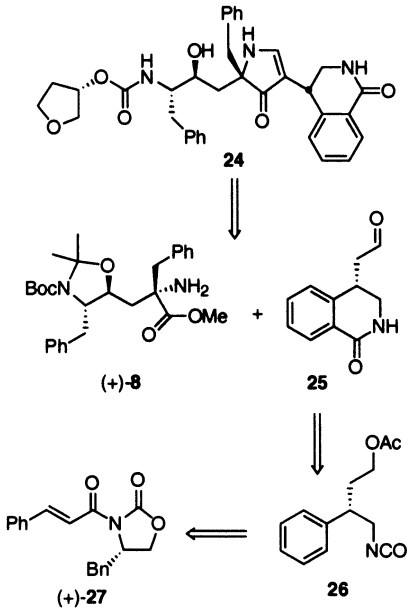

To generate the tetrahydroisoquinolyl framework of **24**, we envisioned the use of a modified Bischeler−Napieralski cyclization. Our initial plan called for a carbamate as the cyclization precursor. However, low yields in this reaction led us to exploit an intramolecular Friedel−Crafts acylation tactic, employing an isocyanate.[40] The required stereogenic center in **25** would be installed prior to cyclization, via diastereoselective conjugate addition of an allyl nucleophile to cinnamic acid derivative (+)-**27**.[41]

In the event, treatment of (+)-**27** with allylMgCl/CuBr·DMS[42] provided (+)-**28**[43] as a single diastereomer (84%) after recrystallization (Scheme 6). Reductive removal of the chiral auxiliary then furnished alcohol (+)-**29**, which in turn was protected as acetate (+)-**30**. Oxidative cleavage of the olefin (RuO_2/$NaIO_4$) led to acid (+)-**31** in good yield, which was in turn converted to the isocyanate (**26**) via Curtius rearrangement. The requisite intramolecular Friedel−Crafts cyclization was achieved by exposure of **26** to $AlCl_3$ at 60 °C to furnish lactam (+)-**32** in moderate yield for the three steps. Methanolysis, followed by Swern oxidation provided (+)-**25**, the required aldehyde for pyrrolinone ring construction.

Scheme 6

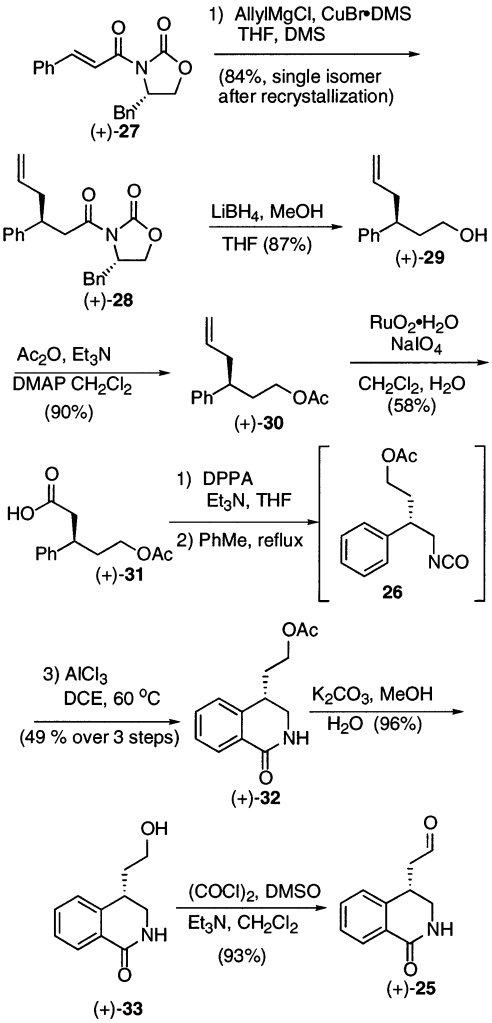

The desired pyrrolinone (+)-**34** (Scheme 7) was prepared in 51% yield via condensation of (+)-**25** with amino ester (+)-**8**, followed by treatment with KHMDS.[44] Conversion to the prospective inhibitor (+)-**24** was then achieved by treatment with TFA/H_2O/CH_2Cl_2 (3 days) to provide an intermediate amino-alcohol, followed by addition of carbonate (+)-**20**;[27] the overall yield was 76%. Pleasingly, (+)-**24** proved to be highly

Scheme 7

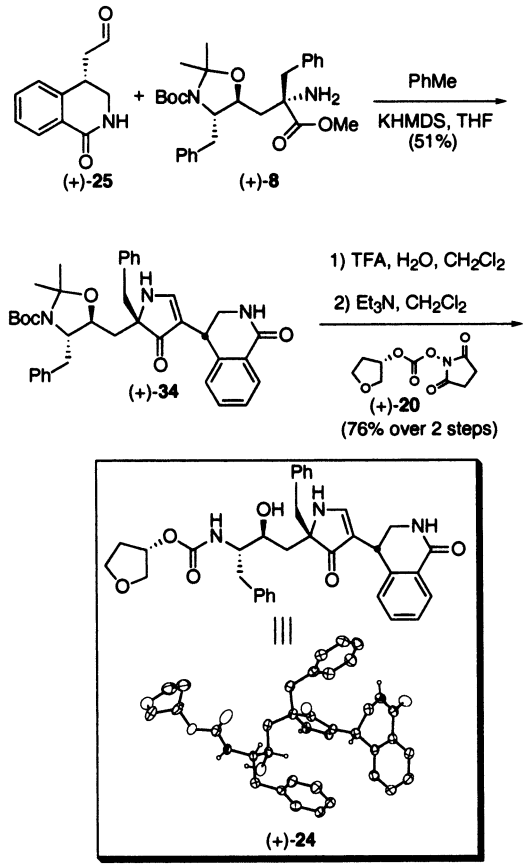

crystalline, thereby permitting confirmation of both the structure and the stereochemistry by single-crystal X-ray analysis.

Biological assay of (+)-**24** revealed an IC_{50} of 5.3 nM and CIC_{95} of 781 nM (C/I, 137, Table 1). Surprised by the modest decrease (2.5-fold) in binding affinity with respect to (−)-**7** and (−)-**23**, we carried out the crystal structure of (+)-**24** cocrystallized with wild-type HIV-1 protease (Figure 6).[45] Several unexpected results were observed. First, the tetrahydroisoquinolyl P2 side chain

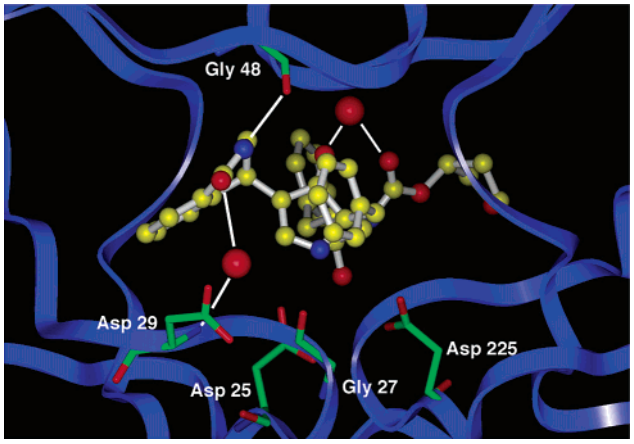

Figure 6. Structure of (+)-**24** cocrystallized with wild-type HIV-1 protease.

had rotated in such a fashion as to create a hydrogen bond between the lactam NH of (+)-**24** and the C=O of Gly48. This orientation, which had not been anticipated by molecular modeling, again created sufficient space in the S2 pocket to include a bridging water molecule between the Asp29 NH and the lactam carbonyl of the inhibitor.

Interpretation of the X-ray Data. We were fortunate to obtain X-ray structures of the three inhibitors [i.e., (−)-**7**, (−)-**23**, and (+)-**24**] complexed with HIV-1 protease, and we anticipated that comparing the positions of the individual inhibitors within the active site and the resultant structural changes of the HIV-1 enzyme might provide an explanation for the observed binding affinities. To this end, superposition of the structures of the inhibitor−enzyme complexes revealed that the P2′-P1 sections of the three inhibitors were in nearly identical orientations, producing similar hydrogen-bonding interactions with the active site. In addition, the P2 side chains of (−)-**7** and (−)-**23** also possessed nearly identical orientations, whereas the P2 side chain of (+)-**24** had rotated toward the flap region of the enzyme. This difference in side chain orientation may account for the modest decrease in the binding affinity of (+)-**24**, by forcing a small change in the position of the enzyme backbone through steric repulsion in the S2 pocket (vide infra).

To assess the changes in the position of the enzyme backbone, we overlayed the enzymes from the three inhibitor−HIV-1 protease crystal structures and that of the Indinavir−enzyme complex (Figure 7).[46] A com-

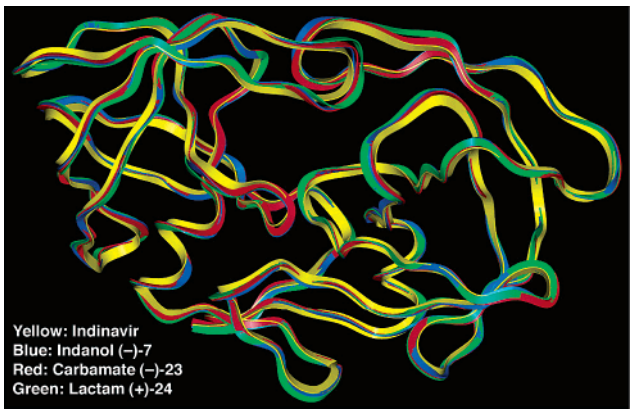

Figure 7. Overlay of the enzyme structures from the three inhibitor−HIV-1 protease crystal structures and that of the Indinavir−enzyme complex.

mon characteristic of the pyrrolinone−HIV-1 protease complexes is seen in the rotation of the carboxylate of Asp225 in order to form a hydrogen bond with the pyrrolinone NH. This conformation is in stark contrast with the complexes with inhibitors such as Indinavir in which the catalytic diad (Asp25/Asp225) generates a hydrogen bond with the hydroxyl transition state mimic. In addition, we observed changes in the backbone position of the loops containing Ile50 and Ile250, when comparing (+)-**24** to (−)-**7** or to (−)-**23**. This conformational change is believed to be due to the steric repulsion generated by the unexpected orientation of the P2 side chain or perhaps to a change in the orientation of the enzyme to generate a hydrogen bond with the NH of the lactam. Significantly, the overall conformation of the complex of (−)-**23** with the HIV-1 protease is the closest to that observed for Indinavir. Although some differences are present, they are small as compared to the conformations of complexes (−)-**7** and (+)-**24** with the

HIV-1 protease. This similarity may be the result of the water molecule, which cocrystallized with (−)-**7** and (+)-**24** but not with (−)-**23** and Indinavir.

Potency Against Mutant Strains of the HIV-1 Protease. Having defined differences in the interactions of the monopyrrolinone inhibitors with the wild-type HIV-1 protease relative to Indinavir, we were intrigued by the possibility that the different binding orientations might enhance the susceptibility of HIV-1 mutant proteases to the monopyrrolinone inhibitors.

When assayed against HIV-1 protease mutant 228,[47] monopyrrolinone inhibitors (−)-**7** and (−)-**23** displayed IC_{50} values of 129 and 364 nM, respectively, while Indinavir displayed an IC_{50} of 288 nM. We then assayed inhibitor (+)-**24**, whose complex with HIV-1 protease showed the most significant changes relative to that of Indinavir, against two different HIV-1 protease mutants, 1002-60 and 2006-18.[28] Inhibitor (+)-**24** displayed an IC_{50} value of 33 nM against mutant 1002-60 and 36 nM against mutant 2006-18, while Indinavir displayed values of 61 and 41 nM, respectively. Importantly, while we cannot directly compare the results from the three mutant enzyme assays, the pyrrolinone-based inhibitors displayed good activity against these mutant enzymes. That the monopyrrolinone-based inhibitor (+)-**24** can maintain efficacy against several mutant strains of the enzyme may be due to the different binding conformations.

Summary and Conclusions

The design, synthesis, and biological evaluation of a series of monopyrrolinone HIV-1 protease inhibitors have been achieved. Importantly, this work validated our initial proposition that use of a monopyrrolinone scaffold would lead to inhibitors with improved bioavailability relative to both their peptidal counterparts and our first generation bispyrrolinone inhibitors. Pleasingly, our most potent monopyrrolinone inhibitor (−)-**7** displays 13% oral bioavailability in dogs.

Detailed information about the interactions between pyrrolinone-based inhibitors and enzymes was obtained via the X-ray crystal structures of the inhibitor−wild-type HIV-1 protease complexes. In particular, all inhibitors displayed similar orientations of the P2′-P1 substituents, along with an unexpected hydrogen bond between the pyrrolinone NH and the enzyme Asp225. Interactions with the S2 pocket were not optimal, as illustrated by inclusion of a water molecule in two of the inhibitor−enzyme complexes. Efforts to increase the observed affinities by displacing this water molecule and establishing a hydrogen bond with Asp29 proved unsuccessful. Lack of success with this venture is a testament to the difficulty of accurately predicting the many variables that influence and build binding affinity. Comparison of the overall macromolecular enzyme conformation between the three complexes and that of Indinavir revealed modest displacements of the protease backbone in the flap region of the enzyme to accommodate the pyrrolinone ring, accompanied by variations in hydrogen bonding. Importantly, the binding orientation of the pyrrolinone-based inhibitors may explain their sustained efficacy against mutant strains of the HIV-1 protease enzyme as compared to Indinavir. Finally, the knowledge gained in these studies holds the promise of a new generation of HIV-1 protease inhibitors possessing improved binding affinity and pharmacokinetic properties.

Experimental Section

General Materials and Methods. All nonaqueous reactions were carried out in oven- or flame-dried glassware under an argon atmosphere and were magnetically stirred. Reactions were monitored by thin-layer chromatography (TLC) with Whatman 0.25 mm precoated silica gel plates unless otherwise noted. Diethyl ether and THF were freshly distilled from sodium/benzophenone under argon and dichloromethane (CH_2Cl_2) from calcium hydride. Triethylamine (TEA), anhydrous pyridine, *N*,*N*-dimethylformamide (DMF), and toluene were purchased anhydrous from Aldrich and used without purification. Except as otherwise indicated, all reagents were purchased and used without purification. *n*-Butyllithium was standardized by titration with diphenylacetic acid. Flash column chromatography was performed using silica gel 60 (particle size 0.023−0.040 mm) supplied by Silicycle, Inc. Yields refer to chromatographically and spectroscopically pure compounds, unless otherwise stated. All melting points were obtained on a Thomas-Hoover apparatus and are corrected. Optical rotations were obtained with a Perkin-Elmer model 241 polarimeter in the solvent indicated at the sodium D line (589 nm) at 25 °C. The values (α) are reported without unit, the latter (deg mL)/(g dm) being implicit. Infrared spectra were recorded on a Perkin-Elmer model 283B spectrometer. Proton, ^1H (500 MHz), and carbon, ^{13}C (125 MHz), NMR spectra were recorded on a Bruker AMX-500, and the chemical shifts were reported relative to solvents. High-resolution mass spectra (HRMS) were obtained at the University of Pennsylvania, Mass Spectrometry Service Center, with either a VG Micromass 70/70H or VG ZAB-E spectrometer. Microanalyses were performed at the University of Pennsylvania. Single-crystal X-ray structure determinations were performed at the University of Pennsylvania with an Enraf Nonius CAD-4 automated diffractometer. Analytical reversed-phased high-performance liquid chromatography (HPLC) was carried out employing a Waters 600E multisolvent delivery system equipped with a 996 photodiodearray detector on a Zorbax 300SB-C18 (4.6 mm × 150 mm, 3.5 μm) column or a Zorbax RX-C8 (4.6 mm × 250 mm, 5 μm) column; preparative reversed-phase HPLC separation was achieved using a Rainin solvent delivery system equipped with a dynamax detector (model UV-D) utilizing a C18 Dynamax 300 Å (21.4 mm × 250 mm) column.

Hydroxysulfoximine (−)-12. A solution of (*R*)-*N*,*S*-dimethyl-*S*-phenylsulfoximine (−)-**11** (8.87 g, 52.4 mmol) in THF (300 mL) was cooled to 0 °C, and *n*-BuLi (2.5 M in hexanes, 22.0 mL, 54.9 mmol) was added dropwise. The reaction mixture was stirred at room temperature for 15 min and then cooled to −78 °C. A solution of cyclobutanone (±)-**10** (7.90 g, 49.9 mmol) in THF (50 mL) was added, and the solution was stirred for 45 min and poured into a saturated solution of NH_4Cl (300 mL). The aqueous layer was extracted with Et_2O (3 × 200 mL), and the combined extracts were washed with water (200 mL) and then brine (200 mL). The organic layer was dried ($MgSO_4$), filtered, and concentrated in vacuo. The resulting 1:1 mixture of diastereomers proved inseparable by flash chromatography or HPLC. Fractional recrystallization from EtOAc/hexanes, however, afforded hydroxysulfoximines (−)-**12** (6.05 g, 37% yield) along with a second diastereomer (6.43 g, 39% yield), both in better than 15:1 diastereomeric purity (^1H NMR) as white crystalline solids. The desired diastereomer (−)-**12**: mp 127−128.5 °C; $[\alpha]_D$ −207 (*c* 0.99, $CHCl_3$). IR ($CDCl_3$): 3200 (br m), 3000 (m), 1475 (m), 1440 (m), 1240 (s), 1150 (s), 1080 (m) cm^{-1}. ^1H NMR (500 MHz, $CDCl_3$): δ 7.88 (m, 2H), 7.66−7.58 (m, 3H), 7.24 (m, 1H), 7.15−7.10 (m, 3H), 6.72 (br s, 1H), 3.57−3.46 (m, 3H), 3.40 (br d, J = 13.9 Hz, 1H), 3.00 (ddd, J = 2.3, 8.7, 13.1 Hz, 1H), 2.89 (ddd, J = 0.9, 9.9, 16.8 Hz, 1H), 2.78−2.74 (m, 1H), 2.63 (s, 3H), 2.15 (app dd, J = 5.3, 13.1, 1H). ^{13}C NMR (125 MHz, $CDCl_3$): δ 146.8, 144.9, 138.5, 133.2, 129.5, 129.1, 126.4,

126.3, 124.5, 123.7, 70.4, 64.6, 48.2, 43.2, 38.4, 31.8, 28.7. HRMS for mixture of diastereomers (CI, NH_3): *m/z* 328.1370 [$(M + H)^+$; calcd for $C_{19}H_{22}NO_2S$, 328.1371; $\sigma = 1$ ppm]. Anal. calcd for $C_{19}H_{21}NO_2S$: C, 69.68; H, 6.48; N, 4.28. Found: C, 69.39; H, 6.24; N, 4.24; X-ray.

Cyclobutanone (−)-13. Hydroxysulfoximine (−)-**12** (3.50 g, 10.7 mmol) was dissolved in toluene (150 mL), and the resulting mixture was heated at reflux under argon for 30 h. The reaction mixture was concentrated in vacuo, and the residue was purified by flash chromatography (8% EtOAc/hexanes and then 100% EtOAc) to afford cyclobutanone (−)-**13** (1.61 g, 95% yield) as a waxy white solid and recovered sulfoximine (1.62 g, 96% yield): mp 44−45 °C; $[\alpha]_D$ −349 (*c* 1.03, $CHCl_3$). IR ($CHCl_3$): 3000 (m), 1780 (s), 1480 (m), 1455 (m), 1390 (m), 1210 (m), 1090 (m) cm^{-1}. ^1H NMR (500 MHz, $CDCl_3$): δ 7.33 (m, 1H), 7.29−7.24 (m, 3H), 4.10−4.07 (m, 2H), 3.66−3.61 (m, 1H), 3.34 (d, $J = 16.9$ Hz, 1H), 3.16−3.11 (m, 1H), 2.94−2.90 (m, 1H). ^{13}C NMR (125 MHz, $CDCl_3$): δ 211.9, 144.5, 143.0, 127.3, 125.3, 125.0, 62.7, 55.6, 55.5, 36.5, 33.9. HRMS (CI, NH_3): *m/z* 159.0813 [$(M + H)^+$; calcd for $C_{11}H_{11}O$, 159.0810; $\sigma = 2$ ppm]. Anal. calcd for $C_{11}H_{10}O$: C, 83.50; H, 6.38. Found: C, 83.37; H, 6.44.

Lactone (−)-14. A solution of cyclobutanone (−)-**13** (1.39 g, 8.79 mmol) in 90% AcOH/water (30 mL) was treated with 30% H_2O_2 (0.896 g, 26.33 mmol) in 90% AcOH/water (16 mL). The resulting mixture was stirred at 5 °C for 20 h, diluted with water (50 mL), and extracted with Et_2O (3 × 60 mL). The combined organic phases were washed with 10% $NaHSO_3$ (2 × 50 mL), saturated $NaHCO_3$ (2 × 50 mL), and brine (50 mL). The organic phase was dried ($MgSO_4$), filtered, and concentrated in vacuo. No further purification of the product was required to yield (−)-**14** (1.38 g, 90%) as a white solid: mp 71−73 °C; $[\alpha]_D$ −71.5 (*c* 1.02, $CHCl_3$). IR ($CHCl_3$): 3020 (m), 1770 (s), 1170 (s), 1140 (m), 1035 (m), 1005 (m). ^1H NMR (500 MHz, $CDCl_3$): δ 7.30−7.24 (m, 4H), 5.31 (m, 1H), 4.05−4.01 (m, 1H), 3.34 (d, $J = 3.3$ Hz, 2H), 3.06 (dd, $J = 9.3$, 17.8 Hz, 1H), 2.76 (dd, $J = 1.5$, 17.8 Hz, 1H). ^{13}C NMR (125 MHz, $CDCl_3$): δ 176.2, 142.0, 140.0, 128.2, 127.7, 125.2, 124.6, 84.2, 45.4, 38.9, 35.3. HRMS (CI, NH_3): *m/z* 174.0680 [M^+ calcd for $C_{11}H_{10}O_2$, 174.0681; $\sigma = 1$ ppm]. Anal. calcd for $C_{11}H_{10}O_2$: C, 75.83; H, 5.80. Found: C, 75.68; H, 5.76.

Amide (−)-15. To a solution of L-2-phenethylamine (6.78 mL, 54.1 mmol) in THF (50 mL) was added dropwise Me_3Al (26.6 mL, 53.2 mmol, 2.0 M solution in hexanes) at room temperature, and the solution was stirred for 50 min, and then, a solution of racemic lactone **14**[23a] (3.08 g, 17.7 mmol) in THF (10 mL) was added. The solution was stirred for 18 h, the reaction was quenched with a saturated solution of Rochelle's salt (50 mL), and the product was extracted with Et_2O (3 × 75 mL). The combined organic phases were washed with a saturated solution of Rochelle's salt (2 × 25 mL), dried (Na_2SO_4), filtered, and concentrated in vacuo. Flash chromatography (3:1, hexanes/EtOAc) furnished (−)-**15** (2.49 g, 48%) and (−)-**16** (2.51, 48%) as colorless crystalline solids.

Amide (−)-15. mp 120−122 °C; $[\alpha]_D$ −27.0 (*c* 0.52, CH_2Cl_2). IR ($CHCl_3$): 3440 (m), 3320 (m), 3010 (m), 2945 (m), 1650 (s), 1520 (s), 1450 (m) cm^{-1}. ^1H NMR (500 MHz, $CDCl_3$): δ 7.33−7.27 (m, 2H), 7.26−7.22 (m, 1H), 7.20−7.14 (m, 5H), 7.11−7.03 (m, 1H), 6.17 (d, $J = 7.6$ Hz, 1H), 5.12−5.06 (m, 1H), 4.67−4.53 (m, 1H), 3.75 (d, $J = 5.5$ Hz, 1H), 3.51−3.47 (m, 1H), 3.14 (dd, $J = 6.4$, 16.6 Hz, 1H), 2.90 (dd, $J = 3.7$, 16.5 Hz, 1H), 2.70 (dd, $J = 4.6$, 14.0 Hz, 1H), 2.62 (dd, $J = 9.8$, 13.9 Hz, 1H), 1.48 (d, $J = 6.9$ Hz, 3H). ^{13}C NMR (125 MHz, $CDCl_3$): δ 172.1, 143.1, 142.8, 141.0, 128.7, 127.3, 127.2, 126.7, 126.0, 125.1, 123.72, 73.71, 50.0, 47.2, 40.6, 36.3, 21.7. HRMS (CI^+): *m/z* 296.1641 [(M^+); calcd for $C_{19}H_{21}NO_2$, 296.1650].

Amide (−)-16. mp 142−144 °C; $[\alpha]_D$ −52.9 (*c* 0.38, CH_2Cl_2). IR ($CHCl_3$): 3440 (w), 3360 (w), 3010 (m), 2980 (m), 1735 (s), 1655 (s), 1515 (m), 1380 (s), 1250 (s), 1050 (s) cm^{-1}. ^1H NMR (500 MHz, $CDCl_3$): δ 7.35−7.31 (m, 2H), 7.29−7.24 (m, 3H), 7.20 (d, $J = 6.6$ Hz, 1H), 7.18−7.12 (m, 2H), 7.06 (d, $J = 7.1$ Hz, 1H), 6.20 (d, $J = 7.5$ Hz, 1H), 5.10−5.07 (m, 1H), 4.68−4.65 (m, 1H), 3.82 (d, $J = 5.4$ Hz, 1H), 3.49−3.45 (m, 1H), 3.15 (dd, $J = 6.3$, 16.5 Hz, 1H), 2.92 (dd, $J = 3.6$, 16.5 Hz, 1H), 2.68−2.60 (m, 2H), 1.40 (d, $J = 7.0$ Hz, 3H). ^{13}C NMR (125 MHz, $CDCl_3$): δ 172.1, 143.1, 142.9, 140.9, 128.7, 127.4, 127.2, 126.7, 126.1, 125.1, 123.7, 73.8, 48.9, 47.1, 40.6, 36.2, 21.5. HRMS (CI^+): *m/z* 296.1643 [$(M + H)^+$; calcd for $C_{19}H_{21}NO_2$, 296.1650].

Lactone (−)-14. To a solution of amide (−)-**15** (3.6 g, 12.2 mmol) in CH_2Cl_2 (100 mL) was added *p*-TSA·H_2O (2.3 g, 12.2 mmol). After it was stirred for 24 h, the mixture was diluted with a 5% solution of citric acid (25 mL), the organic phase was separated, and the aqueous phase was extracted with CH_2Cl_2 (2 × 25 mL). The combined organic phases were then washed with 5% citric acid and saturated $NaHCO_3$, dried ($MgSO_4$), filtered, and concentrated in vacuo. The residue was purified by column chromatography (3:1, hexanes/EtOAc) to give (−)-**14** (2.12 g, 100%) as a white crystalline solid, identical to that prepared above.

TBS-Protected Hydroxyamide (+)-17. A solution of lactone (−)-**14** (1.20 g, 6.89 mmol) in benzene (70 mL) was treated with a stock solution of trimethyl aluminum and *N*,*O*-dimethylhydroxylamine [MeClAlN(OMe)Me] (0.67 M in benzene, 20.6 mL, 13.8 mmol) and stirred for 16 h. The reaction mixture was then added to a saturated solution of Rochelle's salt (250 mL), and Et_2O (200 mL) was added. The phases were separated, and the aqueous phase was extracted with ether (3 × 200 mL). The combined organic phases were washed with a saturated solution of Rochelle's salt (200 mL) and then dried ($MgSO_4$), filtered, and concentrated in vacuo. The resultant hydroxyamide (1.54 g, 6.54 mmol) was then dissolved in CH_2Cl_2, cooled to −78 °C, and treated with 2,6-lutidine (1.14 mL, 9.82 mmol) and TBSOTf (2.25 mL, 9.82 mmol). The resulting mixture was stirred at −78 °C for 30 min and then added to a solution of water (150 mL) and brine (50 mL). The aqueous layer was extracted with Et_2O (2 × 250 mL), and the combined organic phases were washed with a 10% solution $NaHSO_4$ (2 × 200 mL), saturated $NaHCO_3$ (200 mL), and brine (200 mL), dried ($MgSO_4$), filtered, and concentrated in vacuo. Flash chromatography (15−20% EtOAc/hexanes gradient) furnished (+)-**17** (2.02 g, 84% yield for two steps) as a colorless oil: $[\alpha]_D + 4.2$ (*c* 1.0, $CHCl_3$). IR ($CHCl_3$): 2975 (m), 2965 (m), 1650 (s), 1470 (m), 1460 (m), 1380 (m), 1250 (m), 1110 (s), 1065 (m), 1000 (m), 830 (s) cm^{-1}. ^1H NMR (500 MHz, $CDCl_3$): δ 7.21−7.12 (m, 4H), 4.73 (app q, $J = 6.1$ Hz, 1H), 3.69 (app q, $J = 7.1$ Hz, 1H), 3.55 (br s, 3H), 3.18 (s, 3H), 3.06 (dd, $J = 6.3$, 15.7 Hz, 1H), 2.95 (dd, $J = 7.2$, 16.8 Hz, 1H), 2.86 (dd, $J = 5.5$, 15.7 Hz, 1H), 2.64 (dd, $J = 6.6$, 16.4 Hz, 1H), 0.87 (s, 9H), 0.09 (s, 3H), 0.06 (s, 3H). ^{13}C NMR (125 MHz, $CDCl_3$): δ 174.0, 144.4, 140.4, 126.8, 126.4, 124.6, 124.4, 74.7, 61.0, 45.1, 40.8, 32.1 (br), 30.9, 25.9, 18.1, −4.7, −4.9. HRMS (CI, NH_3): *m/z* 350.2138 [$(M + H)^+$; calcd for $C_{19}H_{32}NO_3Si$, 350.2151; $\sigma = 3$ ppm]. Anal. calcd for $C_{19}H_{31}NO_3Si$: C, 65.27; H, 8.96; N, 4.01. Found: C, 65.27; H, 9.04; N, 3.90.

TBS-Protected Hydroxyaldehyde (−)-9. To a solution of (+)-**17** (2.0 g, 5.73 mmol) in THF (45 mL) at −78 °C was added DIBAL dropwise (1.0 M in hexane, 6.32 mL, 6.32 mmol). After 45 min, MeOH (1 mL) was carefully added and the mixture was poured into a saturated solution of Rochelle's salt. The aqueous phase was extracted with Et_2O (3 × 25 mL), and the combined organic phases were dried ($MgSO_4$), filtered, and concentrated in vacuo. Flash chromatography (9:1 hexanes/EtOAc) afforded (−)-**9** (1.53 g, 92% yield) as a colorless oil: $[\alpha]_D$ −39.9 (*c* 1.04, $CHCl_3$). IR ($CHCl_3$): 2960 (s), 2930 (s), 2890 (s), 2860 (s), 1725 (s) cm^{-1}. ^1H NMR (500 MHz, $CDCl_3$): δ 9.88 (s, 1H), 7.17 (m, 4H), 4.71 (q, $J = 6.3$ Hz, 1H), 3.71 (q, $J = 6.2$ Hz, 1H), 3.07 (dd, $J = 6.5$, 15.7 Hz, 1H), 2.97 (dd, $J = 8.1$, 17.5 Hz, 1H), 2.88 (dd, $J = 6.0$, 15.7 Hz, 1H), 2.56 (dd, $J = 5.7$, 17.5 Hz, 1H), 0.87 (s, 9H), 0.09 (s, 3H), 0.07 (s, 3H). ^{13}C NMR (125 MHz, $CDCl_3$): δ 202.1, 143.5, 140.2, 127.1, 126.8, 124.8, 124.1, 74.4, 44.4, 43.2, 40.5, 25.8, 18.1, −4.7, −5.0. HRMS (CI, NH_3): *m/z* 291.1793 [$(M + H)^+$; calcd for $C_{17}H_{27}O_2Si$, 291.1780; $\sigma = 4$ ppm]. Anal. calcd for $C_{17}H_{26}O_2Si$: C, 70.28; H, 9.04. Found: C, 69.96; H, 9.26.

Monopyrrolinone (+)-18. TBS-protected hydroxyaldehyde (−)-**9** (81.4 mg, 0.280 mmol) was combined with aminoester[14b]

(+)-**8** (135.3 mg, 0.280 mmol) in $CHCl_3$ (5 mL), and the solvent was removed in vacuo. The residue was redissolved in dry toluene (3−5 mL) and subsequently concentrated in vacuo with gentle warming for five cycles. The resulting imine was then stored under vacuum for 16 h, dissolved in THF (3 mL), and treated dropwise with KHMDS (0.5 M solution in toluene, 1.68 mL, 0.84 mmol) at room temperature. During the addition, the color of the reaction mixture changed from pale yellow to deep violet. After 10 min, the reaction mixture was quenched with 10% $NaHSO_4$ (10 mL) and the resulting mixture was extracted with EtOAc (2 × 15 mL). The combined organic phases were washed with brine (10 mL), dried ($MgSO_4$), filtered, and concentrated in vacuo. Flash chromatography (5−15% EtOAc/hexanes gradient) afforded (+)-**18** (123.5 mg, 61% yield) as a pale yellow glass: $[\alpha]_D$ + 9.3 (*c* 0.4 $CHCl_3$). IR ($CHCl_3$): 3425 (m), 2960 (m), 2930 (s), 2860 (m), 1685 (s), 1660 (s), 1580 (s), 1390 (s), 1370 (s), 1250 (s), 1170 (s), 1160 (s), 1120 (m), 1090 (s), 1060 (s) cm^{-1}. ^1H NMR (500 MHz, $CDCl_3$, 330 K): δ 7.61 (br d, J = 2.7 Hz, 1H), 7.30−7.09 (m, 14H), 6.95 (br t, J = 7.4 Hz, 1H), 6.72 (br d, J = 7.5 Hz, 1H), 5.17 (br s, 1H), 4.63 (m, 1H), 4.30 (br d, J = 5.1 Hz, 1H), 3.73 (td, J = 1.3, 8.3 Hz, 1H), 3.56 (td, J = 2.2, 6.6 Hz, 1H), 3.15 (dd, J = 5.2, 15.9 Hz, 1H), 2.94 (dd, J = 2.6, 15.9 Hz, 1H), 2.85−2.75 (m, 2H), 2.07 (app br d, J = 12.6 Hz, 1H), 1.79 (dd, J = 9.4, 14.5 Hz, 1H), 1.51 (s, 9H), 1.33 (s, 3H), 0.86 (s, 12H, overlapping singlets), 0.08 (s, 3H), 0.01 (s, 3H). ^{13}C NMR (125 MHz, $CDCl_3$, 330 K): δ 203.2, 164.8, 152.1, 144.6, 141.2, 136.8, 136.6, 130.5, 128.4, 128.3, 126.8, 126.5, 126.5, 126.3, 124.5, 124.5, 112.3, 94.4, 80.0, 75.5, 74.0, 69.1, 63.6, 53.2, 44.7, 43.4, 42.1, 38.8, 28.6, 27.9, 26.0, 25.8, 18.2, −4.4, −4.8. HRMS (FAB, *m*-nitrobenzyl alcohol): *m*/*z* 745.4044 [(M + Na)$^+$; calcd for $C_{44}H_{58}N_2O_5SiNa$, 745.4013].

Monopyrrolinone (+)-19. Monopyrrolinone (+)-**18** (161 mg, 0.223 mmol) was dissolved in 1 N anhydrous methanolic HCl (22 mL), and the resulting solution was stirred at room temperature for 4.5 h. Solid $NaHCO_3$ was then added portionwise until the evolution of gas ceased. Most of the methanol was then removed in vacuo, and the residue was dissolved in a mixture of EtOAc (30 mL) and saturated $NaHCO_3$ (30 mL). The phases were separated, and the aqueous phase was extracted with EtOAc (2 × 30 mL). The combined organic phases were then washed with brine (30 mL), dried ($MgSO_4$), filtered, and concentrated in vacuo. Flash chromatography (6% MeOH-saturated with NH_3/CH_2Cl_2) furnished (+)-**19** (95 mg, 91% yield) as a white solid: mp 74 °C (dec); $[\alpha]_D$ + 3.8 (*c* 0.99, $CHCl_3$). IR ($CHCl_3$): 3570 (m), 3450 (m), 3400 (br m), 3300 (br m), 2920 (m), 1650 (s), 1570 (s), 1460 (m), 1170 (m), 900 (br s), 730 (br s) cm^{-1}. ^1H NMR (500 MHz, $CDCl_3$): 7.56 (s, 1H), 7.31 (t, J = 7.6 Hz, 2H), 7.28−7.18 (m, 9H), 7.14 (t, J = 7.4 Hz, 1H), 7.09 (t, J = 7.3 Hz, 1H), 6.99 (br s, 1H), 6.77 (d, J = 7.4 Hz, 1H), 4.24 (td, J = 4.9, 1.3 Hz, 1H), 4.07 (d, J = 4.6 Hz, 1H), 3.57−3.54 (m, 1H), 3.16 (d, J = 13.1 Hz, 1H), 3.04 (dd, J = 5.1, 16.3 Hz, 1H), 2.98 (d, J = 13.2 Hz, 1H), 3.00−2.96 (m, overlapping with another signal, 1H), 2.90 (m, 1H), 2.86 (d, J = 16.3 Hz, 1H), 2.55 (dd, J = 9.1, 13.5 Hz, 1H), 2.24 (dd, J = 2.5, 14.4 Hz, 1H), 2.19 (very br s, ∼4H), 2.02 (dd, J = 9.0, 14.4 Hz, 1H). ^{13}C NMR (125 MHz, $CDCl_3$): δ 203.8, 165.0, 142.6, 141.6, 138.5, 135.1, 130.1, 129.2, 128.6 127.8, 127.1, 126.7, 126.5, 126.4, 124.9, 124.1, 109.8, 74.2, 70.6, 69.8, 57.0, 45.7, 43.6, 40.9, 40.5, 40.4. HRMS (CI, NH_3): *m*/*z* 469.2489 [(M + H)$^+$; calcd for $C_{30}H_{33}N_2O_3$, 469.2490; σ = 1 ppm].

Boc-Monopyrrolinone Inhibitor (−)-6. A solution of free amine (+)-**19** (13.0 mg, 0.0277 mmol) in CH_2Cl_2 (1 mL) was treated with $(Boc)_2O$ (7.2 mg, 0.033 mmol) and Et_3N (0.0097 mL, 0.069 mmol), and the resultant solution was stirred at room temperature for 2.5 h. The reaction was then quenched with 10% $NaHSO_4$ (5 mL), and the mixture was extracted with EtOAc (2 × 8 mL). The combined organic phases were then washed with 10% $NaHSO_4$ (5 mL), saturated $NaHCO_3$ (5 mL), and brine (5 mL), dried ($MgSO_4$), filtered, and concentrated in vacuo. Flash chromatography (45−65% EtOAc/hexanes, gradient) afforded (−)-**6** (13.5 mg, 86% yield) as a white solid: mp 212−213 °C; $[\alpha]_D$ −26 (*c* 1.0, $CHCl_3$). IR ($CHCl_3$): 3560 (m), 3440 (m), 3280 (br m), 3000 (m), 1680 (s), 1490 (s), 1160 (s), 900 (s) cm^{-1}. ^1H NMR (500 MHz, $CDCl_3$, 330 K): δ 7.49 (s, 1H), 7.30−7.04 (m, 14H), 6.79 (br d, J = 7.3 Hz, 1H), 6.34 (br s, 1H), 5.03 (br d, J = 9.1 Hz, 1H), 4.24 (m, 1H), 4.06 (d, J = 4.6 Hz, 1H), 4.00 (br d, J = 8.9 Hz, 1H), 3.65 (q, J = 7.7 Hz, 1H), 3.13 (d, J = 13.2 Hz, 1H), 3.03 (dd, J = 16.3, 5.0 Hz, 1H), 2.95 (m, 2H), 2.84−2.80 (m, 2H), 2.01 (dd, J = 14.2, 9.4 Hz, 1H), 1.90 (br d, J = 12.6 Hz, 1H), 1.40 (s, 9H). ^{13}C NMR (125 MHz, $CDCl_3$, 330 K): δ 204.4, 164.4, 156.6, 142.6, 141.7, 138.5, 134.9, 130.2, 129.5, 128.6, 128.1, 127.3, 127.0, 126.5, 126.5, 125.0, 124.2, 110.4, 79.7, 74.3, 70.6, 68.2, 57.5, 45.5, 42.2, 40.5, 40.5, 38.9, 28.4. HRMS (FAB, *m*-nitrobenzyl alcohol): *m*/*z* 591.2848 [(M + Na)$^+$; calcd for $C_{35}H_{40}N_2O_5Na$, 591.2835]. Anal. calcd for $C_{35}H_{40}N_2O_5$: C, 73.91; H, 7.10; N, 4.93. Found: C, 73.59; H, 7.19; N, 4.70.

Tetrahydrofuranylcarbamate-Monopyrrolinone (−)-7. A solution of free amine (+)-**19** (170 mg, 0.363 mmol) in CH_2Cl_2 (10 mL) was treated with tetrahydrofuranylsuccidimidyl carbonate (+)-**20** (104 mg, 0.453 mmol) and Et_3N (110 mg, 1.09 mmol), and the solution was stirred at room temperature for 6.5 h. The reaction was quenched with CH_2Cl_2 (30 mL) and 10% $NaHSO_4$ (30 mL), and the resultant phases were separated. The organic layer was washed again with 10% $NaHSO_4$ (30 mL). The combined aqueous phases were extracted with CH_2Cl_2 (2 × 30 mL), and the combined organic phases were washed with saturated $NaHCO_3$ (30 mL) and brine (30 mL), dried ($MgSO_4$), filtered, and concentrated in vacuo. Flash chromatography (80−90% EtOAc/hexanes, gradient) furnished (−)-**7** (183 mg, 87% yield) as a pale yellow glass: $[\alpha]_D$ −55 (*c* 0.18, $CHCl_3$). IR ($CHCl_3$): 3700 (m), 3440 (m), 3350 (br m), 3020 (m), 1715 (s), 1360 (m), 1210 (s) cm^{-1}. ^1H NMR (500 MHz, $CDCl_3$, 330 K): δ 7.54 (s, 1H), 7.32−7.17 (m, 10H), 7.13 (t, J = 7.3 Hz, 1H), 7.08 (t, J = 7.3 Hz, 1H), 7.03 (d, J = 6.6 Hz, 2H), 6.77 (d, J = 7.4 Hz, 1H), 6.29 (br s, 1H), 5.17−5.12 (m, 2H), 4.31 (m, 1H), 4.07−4.03 (m, 2H), 3.90−3.76 (m, 4H), 3.7 (m, 2H), 3.14 (d, J = 13.4 Hz, 1H), 3.05 (dd, J = 5.2, 16.3 Hz, 1H), 2.98 (dd, J = 7.8, 13.6 Hz, 1H), 2.93−2.80 (m, 3H), 2.10 (app br s, 1H), 2.03−1.89 (m, 3H). ^{13}C NMR (125 MHz, $CDCl_3$, 330 K): δ 204.7, 164.3, 156.5, 142.5, 141.6, 138.3, 134.8, 130.1, 129.5, 128.6, 128.2, 127.4, 127.0, 126.6, 126.6, 125.1, 124.2, 110.8, 75.5, 74.3, 73.3, 70.6, 67.9, 67.0, 57.9, 45.5, 42.3, 40.5, 40.4, 38.9, 32.8. HRMS (CI, NH_3): *m*/*z* 583.2802 [(M + H)$^+$; calcd for $C_{35}H_{39}N_2O_6$, 583.2808; σ = 1 ppm].

Indanol (+)-21. To a solution of pyrrolinone (+)-**18** (83 mg, 0.115 mmol) in THF (1 mL) at room temperature was added TBAF (0.23 mL, 0.23 mmol, 1.0 M solution in THF). After it was stirred for 24 h, saturated NH_4Cl (1 mL) was added and the reaction mixture was poured into EtOAc (2 mL). The aqueous phase was then extracted with EtOAc (2 × 3 mL), the combined organic extracts were dried ($MgSO_4$), filtered, and concentrated in vacuo. Flash chromatography (50% EtOAc: hexanes) afforded (+)-**21** (53 mg, 76%) as a white amorphous solid: $[\alpha]_D$ + 14.7 (*c* 1.00, $CHCl_3$). IR ($CHCl_3$): 3560 (w), 3420 (w), 3002 (w), 2980 (s), 2920 (m), 1680 (s), 1665 (s), 1575 (s), 1395 (s), 1380 (s), 1370 (s), 1200 (m), 1170 (m), 1120 (m), 1080 (m), 1040 (w), 700 (s) cm^{-1}. ^1H NMR (500 MHz, $CDCl_3$): δ 7.38 (d, J = 3.6 Hz, 1H), 7.30−7.10 (m, 14H), 7.00 (t, J = 7.1 Hz, 1H), 6.58 (d, J = 7.2 Hz, 1H), 5.40 (apparent bs, 1H), 4.15 (m, 2H), 3.80 (dd, J = 7.1, 6.7 Hz, 1H), 3.75 (bm, 1H), 3.38 (bm, 1H), 3.05 (m, 2H), 2.90 (m, 1H), 2.84 (s, 1H), 2.80 (d, J = 4.7 Hz, 1H), 2.38−2.12 (br m, 1H), 2.20 (dd, J = 8.4, 14.6 Hz, 1H), 1.58 (s, 12H), 1.12−0.88 (br m, 3H). ^{13}C NMR (125 MHz, $CDCl_3$): δ 202.8, 164.6, 142.4, 141.9, 136.7, 135.0, 130.1, 128.4, 127.8, 127.2, 126.8, 126.3, 124.9, 124.2, 111.2, 80.2, 73.5, 70.2, 63.2, 45.4, 43.3, 40.2, 28.5, 25.7. HRMS (Cl, NH_3): *m*/*z* 609.3316 [(M + H)$^+$; calcd for $C_{38}H_{45}N_2O_5$, 609.3328; σ = 2 ppm].

Trichloroacetyl Carbamate (+)-22. To a solution of indanol (+)-**18** (67 mg, 0.110 mmol) in CH_2Cl_2 (1 mL) at room temperature was added trichloroacetylisocyanate (0.013 mL, 0.110 mmol), and after 1 h, the solvent was removed in vacuo. Flash chromatography (5−25% EtOAc:hexanes, gradient) furnished (+)-**22** (67 mg, 76%) as a colorless oil; $[\alpha]_D$ + 7.0 (*c* 1.00, $CHCl_3$). IR ($CHCl_3$): 3680 (w), 3540 (w), 3450 (m), 3010

(m), 2960 (s), 2920 (m), 1735 (s), 1680 (s), 1665 (s), 1580 (s), 1390 (s), 1380 (s), 1370 (s), 1325 (w), 1200 (s), 710 (s) cm^{-1}. ^1H NMR (500 MHz, $CDCl_3$): δ 7.80 (bs, 1H), 7.67 (d, J = 3.9 Hz, 1H), 7.26−7.02 (m, 14H), 6.62 (d, J = 7.4 Hz, 1H), 5.38 (d, J = 3.6 Hz, 1H), 5.29 (s, 1H), 4.47 (br s, 1H), 3.78 (t, J = 7.1 Hz, 1H), 3.67 (br s, 1H), 3.27 (dd, J = 4.5, 17.1 Hz, 1H), 3.08 (d, J = 17.2 Hz, 1H), 2.98 (d, J = 12.2 Hz, 1H), 2.86 (m, 1H), 2.79 (d, J = 13.2 Hz, 1H), 2.33−2.11 (br m, 1H), 1.95 (dd, J = 8.7, 14.5 Hz, 1H), 1.55 (bs, 12H), 1.04−0.83 (br m, 3H). ^{13}C NMR (125 MHz, $CDCl_3$): δ 202.4, 165.1, 156.9, 149.5, 142.7, 139.8, 136.7, 135.2, 130.6, 130.2, 128.3, 127.6, 127.1, 126.8, 126.8, 126.5, 124.7, 124.0, 109.4, 92.0, 81.7, 80.1, 69.7, 63.3, 43.5, 42.4, 38.7, 29.7, 28.5, 28.3, 25.7. HRMS (Cl, NH_3): m/z 818.2142 [$(M + Na)^+$; calcd for $C_{41}H_{45}N_3O_7$, 818.2160; σ = 2.5 ppm].

Carbamate (−)-23. To a solution of (+)-**22** (67 mg, 0.084 mmol) in MeOH (2 mL) was added *p*-TSA (64 mg, 0.34 mmol), and after it was stirred for 72 h, the solvent was removed in vacuo with low heat. The residue was diluted with CH_2Cl_2 (2 mL), saturated $NaHCO_3$ was added, the mixture was stirred for 10 min, and the aqueous phase was extracted with CH_2Cl_2 (2 × 5 mL). The combined organic phases were then dried ($MgSO_4$), filtered, and concentrated in vacuo, and the residue was dissolved in CH_2Cl_2 (1 mL). To this solution were added (+)-**20** (9.8 mg, 0.043 mmol) and Et_3N (0.012 mL, 0.087 mmol). After it was stirred at room temperature for 18 h, the reaction was quenched by adding a mixture of CH_2Cl_2 (2 mL) and 10% $NaHSO_4$ (3 mL), the aqueous phase was extracted with CH_2Cl_2 (2 × 2 mL), and the combined organic phases were dried ($MgSO_4$), filtered, and concentrated in vacuo. Flash chromatography (50−100% EtOAc:hexanes, gradient) afforded (−)-**23** as a white solid (8 mg, 15%): $[\alpha]_D$ − 43 (*c* 0.27, $CHCl_3$). IR ($CHCl_3$): 3440 (m), 3340 (br), 3020 (s), 2940 (m), 1720 (s), 1710 (s), 1640 (w), 1575 (s), 1495 (m), 1330 (w), 1220 (m), 1205 (m), 1085 (s), 1050 (s), 720 (s) cm^{-1}. ^1H NMR (500 MHz, $CDCl_3$, 330 K): δ 7.67 (br s, 1H), 7.36−7.28 (m, 4H), 7.26−7.15 (m, 7H), 6.93 (d, J = 7.1 Hz, 1H), 6.80 (d, J = 7.0 Hz, 2H), 5.46−5.43 (m, 1H), 5.29−5.20 (br, 1H), 5.18−5.13 (br, 1H), 5.12−5.07 (br, 1H), 4.65 (s, 1H), 4.61−4.48 (br, 2H), 4.31 (d, J = 6.0 Hz, 1H), 4.14 (d, J = 8.5 Hz, 1H), 4.00−3.79 (br, 3H), 3.72 (d, J = 9.8 Hz, 1H), 3.69−3.61 (br, 1H), 3.26 (dd, J = 5.9, 16.6 Hz, 1H), 3.15 (br d, J = 15.9 Hz, 1H), 2.98−2.85 (m, 4H), 2.20−2.08 (br, 1H), 2.05−1.94 (br, 1H), 1.81−1.70 (br m, 1H), 1.65 (d, J = 14.4 Hz, 1H). ^{13}C NMR (125 MHz, $CDCl_3$): δ 205.5, 162.5, 156.1, 142.2, 140.6, 138.3, 135.1, 130.0, 129.6, 128.6, 128.4, 127.19, 127.13, 126.8, 126.6, 124.7, 124.1, 109.9, 77.4, 75.3, 73.4, 70.0, 67.1, 67.0, 58.0, 43.6, 40.9, 38.9, 38.8, 38.7, 32.8, 29.6. HRMS (Cl, NH_3): m/z 626.2860 [$(M + H)^+$; calcd for $C_{36}H_{40}N_3O_7$, 628.2866; σ = +1 ppm]. Anal. calcd for $C_{36}H_{39}N_3O_7 \cdot 0.5H_2O$: C, 68.12; H, 6.35; N, 6.62. Found: C, 68.04; H, 6.17; N, 6.23.

Oxazolidinone (+)-28. To a solution of freshly recrystallized CuBr·DMS (2.47 g, 12.0 mmol) in a mixture of THF (110 mL) and DMS (17 mL) at −40 °C was added dropwise allylmagnesium chloride (2 M solution in THF, 23.9 mmol, 11.9 mL). After it was stirred for 30 min, the solution was cooled to −78 °C, and a solution of oxazolidinone (+)-**27**[41] (2.45 g, 7.98 mmol) in THF (110 mL) was added via cannula. After 45 min, the reaction was complete by TLC analysis, saturated NH_4Cl (50 mL) was added, and the mixture was warmed to room temperature. Excess DMS was removed by bubbling air through the reaction mixture (90 min) with the outlet connected to a bleach trap. The aqueous phase was then extracted with EtOAc (3 × 100 mL), and the combined organic phases were dried ($MgSO_4$), filtered, and concentrated in vacuo. Recrystallization from DCM/hexanes (1:10) afforded diastereomerically pure (+)-**28** (2.35 g, 84%) as a white crystalline solid (the initial isomer ratio was >60:1 as measured by ^1H NMR of the crude reaction mixture): mp 90−91 °C; $[\alpha]_D$ + 66.5 (*c* 1.14, $CHCl_3$). IR (neat): 1781 (s), 1699 (s), 1385 (m), 1352 (m), 1210 (m), 1196 (m) cm^{-1}. ^1H NMR (500 MHz, $CDCl_3$): δ 7.33−7.25 (m, 6H), 7.21−7.16 (m, 4H), 5.76−5.68 (m, 1H), 5.05 (d, J = 17.1 Hz, 1H), 5.01 (d, J = 10.2 Hz, 1H), 4.51−4.48 (m, 1H), 4.05 (dd, J = 1.6, 9.0 Hz, 1H), 3.98 (t, J = 8.4 Hz, 1H), 3.44−3.36 (m, 2H), 3.25 (dd, J = 3.1, 14.0 Hz, 1H), 3.20 (dd, J = 3.3, 13.4 Hz, 1H), 2.66 (dd, J = 9.8, 13.4 Hz, 1H), 2.48−2.44 (m, 2H). ^{13}C NMR (125 MHz, $CDCl_3$): δ 171.8, 153.3, 143.6, 136.0, 135.3, 129.3, 128.9, 128.4, 127.7, 127.3, 126.5, 116.9, 66.0, 55.1, 41.4, 41.0, 40.9, 37.8. LRMS (ES^+): 721 (2M + Na), 372 (M + Na). HRMS (ES^+): m/z 372.1586 [$(M + Na)^+$; calcd for $C_{22}H_{23}NO_3Na$, 372.1576; σ = −2.8 ppm]. Anal. calcd for ($C_{22}H_{23}NO_3$): C, 75.62%; H, 6.63%; N, 4.01%. Found: C, 75.61%; H, 6.69%; N, 3.87%.

Alcohol (+)-29. To a solution of oxazolidinone (+)-**28** (2.7 g, 7.74 mmol) in THF (50 mL) were added $LiBH_4$ (2 M solution in THF, 4.26 mL, 8.52 mmol) and MeOH (0.310 mL, 7.74 mmol) at 0 °C. The solution was then stirred at room temperature for 4 h and then NaOH (1 N in H_2O, 25 mL) was added, and the aqueous phase was extracted with Et_2O (3 × 150 mL). The combined organic phases were dried ($MgSO_4$), filtered, and concentrated in vacuo. Flash chromatography (5:1 hexanes/EtOAc) furnished (+)-**29** (1.19 g, 87%) as a colorless oil: $[\alpha]_D$ + 0.3 (*c* 1.1, $CHCl_3$). IR (neat): 3339 (br), 2929 (s), 1494 (m), 1452 (m), 1045 (s), 912 (s) cm^{-1}. ^1H NMR (500 MHz, $CDCl_3$): δ 7.31−7.25 (m, 2H), 7.21−7.16 (m, 3H), 5.70−5.63 (m, 1H), 4.98 (dd, J = 1.2, 17.0 Hz, 1H), 4.94 (dd, J = 1.0, 10.1 Hz, 1H), 3.56−3.51 (m, 1H), 3.48−3.43 (m, 1H), 2.81−2.77 (m, 1H), 2.39 (dt, J = 1.0, 7.2 Hz, 2H), 2.02−1.96 (m, 1H), 1.83−1.77 (m, 1H), 1.39 (br s, 1H). ^{13}C NMR (125 MHz, $CDCl_3$): δ 144.5, 136.7, 128.4, 127.6, 126.3, 116.1, 60.9, 42.2, 41.3, 38.6. LRMS (CI^+): 177 (M + H), 159 (M − OH), 135 (M − allyl). HRMS (CI^+): m/z 176.1195 [$(M)^+$; calcd for $C_{12}H_{16}O$, 176.1201; σ = +3.2 ppm].

Acetate (+)-30. To a solution of alcohol (+)-**29** (1.15 g, 6.53 mmol) in CH_2Cl_2 (50 mL) at 0 °C were added Et_3N (1.10 mL, 7.84 mmol), Ac_2O (0.739 mL, 7.84 mmol), and DMAP (15 mg). After 1 h, a saturated solution of NH_4Cl (25 mL) was added, the aqueous phase was extracted with CH_2Cl_2 (3 × 50 mL), and the combined organic phases were dried (Na_2SO_4), filtered, and concentrated in vacuo. Flash chromatography (95:5 hexanes/EtOAc) afforded (+)-**30** (1.28 g, 90%) as a colorless liquid: $[\alpha]_D$ + 22.3 (*c* 0.91, $CHCl_3$). IR (neat): 1740 (s), 1366 (w), 1239 (s), 1039 (m) cm^{-1}. ^1H NMR (500 MHz, $CDCl_3$): δ 7.31−7.28 (m, 2H), 7.21−7.15 (m, 3H), 5.70−5.62 (m, 1H), 4.97−4.94 (m, 2H), 4.00−3.95 (m, 1H), 3.91−3.86 (m, 1H), 2.78−2.72 (m, 1H), 2.39 (t, J = 7.1 Hz, 2H), 2.07−2.01 (m, 1H), 1.98 (s, 3H), 1.90−1.85 (m, 1H). ^{13}C NMR (125 MHz, $CDCl_3$): δ 170.9, 143.8, 136.4, 128.4, 127.6, 126.4, 116.3, 62.8, 42.5, 41.2, 34.4, 20.8. LRMS (CI^+): 219 (M + H), 177 (M − allyl), 159 (M − OAc). HRMS (CI^+): m/z 219.1378 [$(M + H)^+$; calcd for $C_{14}H_{19}O_2$, 219.1385; σ = +3.2 ppm].

Acid (+)-31. To a solution of alkene (+)-**30** (459 mg, 2.11 mmol) in a mixture of H_2O (11.1 mL), CH_2Cl_2 (7.3 mL), and MeCN (7.3 mL) were added $RuO_2 \cdot H_2O$ (12 mg, 0.093 mmol) and $NaIO_4$ (1.99 g, 9.28 mmol). The mixture was vigorously stirred at room temperature for 3 h, at which point a white precipitate appeared. Additional amounts of $RuO_2 \cdot H_2O$ (12 mg, 0.093 mmol) and $NaIO_4$ (1.99 g, 9.28 mmol) were required, and after 1 h, the reaction was complete. A 1 N aqueous solution of HCl (20 mL) was added, followed by solid Na_2SO_3 in small portions (exothermic), until the reddish/brown color had disappeared. The aqueous phase was then extracted with CH_2Cl_2 (4 × 100 mL), and the combined organic phases were washed with 10% $Na_2S_2O_3$ (100 mL), dried (Na_2SO_4), filtered, and concentrated in vacuo. The residue was then treated with saturated $NaHCO_3$ (30 mL) and washed with CH_2Cl_2 (4 × 20 mL). The aqueous phases were acidified to pH 1 using concentrated HCl and extracted with CH_2Cl_2 (4 × 40 mL), and the combined organic phases were dried (Na_2SO_4), filtered, and concentrated in vacuo to afford (+)-**31** (291 mg, 58%) as a yellowish oil: $[\alpha]_D$ + 12.8 (*c* 0.90, $CHCl_3$). IR (neat): 2922 (br), 1738 (s), 1710 (s), 1238 (s), 1042 (m) cm^{-1}. ^1H NMR (500 MHz, $CDCl_3$): δ 7.31−7.17 (m, 5H), 4.00−3.96 (m, 1H), 3.87−3.82 (m, 1H), 3.26−3.20 (m, 1H), 2.69 (dd, J = 7.3, 15.7 Hz, 1H), 2.65 (dd, J = 7.7, 15.9 Hz, 1H), 2.09−2.02 (m, 1H), 1.98 (s, 3H), 1.95−1.89 (m, 1H). ^{13}C NMR (125 MHz, $CDCl_3$): δ 177.8, 171.1, 142.4, 128.7, 127.3, 126.9, 62.3, 41.1, 38.6, 34.6, 20.8. LRMS (CI^+): 237 (M + H), 219 (M − OH), 177 (M − OAc).

HRMS (CI^+): *m/z* 237.1122 [$(M + H)^+$; calcd for $C_{13}H_{17}O_4$, 237.1127; $\sigma = +1.9$ ppm].

Tetrahydroisoquinolyl Acetate (+)-32. To a solution of acid (+)-**31** (202 mg, 0.856 mmol) in THF (20 mL) were added TEA (0.477 mL, 3.41 mmol) and diphenylphosphoryl azide (0.366 mL, 1.70 mmol). After it was stirred at room temperature for 3 h, water (20 mL) was added, the aqueous phase was extracted with EtOAc (3 × 50 mL), and the combined organic phases were dried ($MgSO_4$), filtered, and concentrated (without heating) in vacuo. Flash chromatography (10:1 hexanes/EtOAc) provided the corresponding acyl azide (159 mg, 71%). This compound was placed under vacuum for 1 h and dissolved with toluene (15 mL), and the solution was heated to 110 °C until the acyl azide had disappeared by IR spectroscopy. Upon completion (∼ 20 min), the solution was cooled and concentrated in vacuo to give isocyanate **26** (142 mg, 100%), which was then placed under vacuum for 1 h. Isocyanate **26** was then dissolved in dichloroethane (40 mL), $AlCl_3$ (323 mg, 2.43 mmol) was added, and the mixture was heated to 60 °C (internal temperature). Heating was maintained for 18 h, during which time the solution turned gradually from yellow to black. The reaction mixture was then cooled to room temperature, and water (18 mL) was slowly added, followed by a 10% aqueous solution of Rochelle's salt (10 mL). The aqueous phase was then extracted with CH_2Cl_2 (4 × 30 mL), and the combined organic phases were dried ($MgSO_4$), filtered, and concentrated in vacuo. Flash chromatography (95:5 CH_2Cl_2/MeOH) furnished (+)-**32** (99 mg, 70%) as a yellow oil: $[\alpha]_D$ + 148 (*c* 1.05, $CHCl_3$). IR (neat): 3252 (br), 2361 (m), 2339 (m), 1736 (s), 1668 (s), 1476 (m), 1239 (s) cm^{-1}. ^1H NMR (500 MHz, $CDCl_3$): δ 8.06 (d, $J = 7.6$ Hz, 1H), 7.46 (t, $J = 7.5$ Hz, 1H), 7.38 (br s, 1H), 7.36 (t, $J = 7.5$ Hz, 1H), 7.19 (d, $J = 7.5$ Hz, 1H), 4.18−4.14 (m, 1H), 4.05−4.00 (m, 1H), 3.76 (dd, $J = 4.1$, 12.5 Hz, 1H), 3.42−3.39 (m, 1H), 3.01−2.99 (m, 1H), 2.05 (s, 3H), 2.04−2.01 (m, 2H). ^{13}C NMR (125 MHz, $CDCl_3$): δ 170.9, 167.4, 141.7, 132.2, 128.3, 127.4, 127.4, 127.0, 61.8, 54.6, 34.6, 32.0, 20.9. LRMS (CI^+): 234 (M + H), 174 (M − OAc). HRMS (CI^+): *m/z* 234.1142 [$(M + H)^+$; calcd for $C_{13}H_{16}NO_3$, 234.1131; $\sigma = -5.0$ ppm].

Alcohol (+)-33. To a solution of acetate (+)-**32** (84 mg, 0.361 mmol) in MeOH (7 mL) and water (0.7 mL) at 0 °C was added K_2CO_3 (52 mg, 0.380 mmol). The solution was stirred for 2.5 h, then citric acid was added (150 mg), and the MeOH was removed in vacuo. The residue was dissolved with EtOAc (120 mL), and the organic phase was washed with saturated $NaHCO_3$ (40 mL) and brine (40 mL), dried (Na_2SO_4), filtered, and concentrated in vacuo. Flash chromatography (10:1 CH_2Cl_2/MeOH) afforded (+)-**33** (66 mg, 96%) as a yellow oil: $[\alpha]_D$ + 178 (*c* 1.33, $CHCl_3$). IR (neat): 3293 (br), 2928 (m), 2873 (m), 1660 (s), 1604 (m), 1475 (m), 1332 (m), 1061 (m) cm^{-1}. ^1H NMR (500 MHz, $CDCl_3$): δ 8.00 (d, $J = 7.6$ Hz, 1H), 7.41 (dt, $J = 1.2$, 7.5 Hz, 1H), 7.31 (dt, $J = 0.5$, 7.5 Hz, 1H), 7.22 (d, $J = 7.5$ Hz, 1H), 6.61 (br s, 1H), 3.71−3.65 (m, 2H), 3.63−3.58 (m, 1H), 3.44−3.40 (m, 1H), 3.14−3.08 (m, 2H) 1.87 (qn, $J = 7.0$ Hz, 2H). ^{13}C NMR (125 MHz, $CDCl_3$): δ 166.5, 142.7, 132.2, 128.0, 128.0, 127.1, 127.1, 59.8, 44.0, 35.8, 34.4. LRMS (CI^+): 192 (M + H). HRMS (CI^+): *m/z* 192.1031 [$(M + H)^+$; calcd for $C_{11}H_{14}NO_2$, 192.1025; $\sigma = -3.1$ ppm].

Aldehyde (+)-25. To a solution of oxalyl chloride (0.050 mL, 0.569 mmol) in CH_2Cl_2 (10 mL) was added DMSO (0.077 mL, 1.10 mmol) at −78 °C, and once the gaseous evolution had ceased, a solution of the alcohol (+)-**33** (75 mg, 0.393 mmol) in CH_2Cl_2 (15 mL) was added via cannula. The mixture was stirred for 30 min before Et_3N (0.208 mL, 1.49 mmol) was added, and this mixture was stirred at 0 °C. After 15 min, saturated NH_4Cl (30 mL) was added, the aqueous phase was extracted with CH_2Cl_2 (3 × 75 mL), and the combined organic phases were dried ($MgSO_4$), filtered, and concentrated in vacuo. Flash chromatography (9:1 EtOAc/MeOH) afforded (+)-**25** as a yellowish oil (69 mg, 93%): $[\alpha]_D$ + 147 (*c* 1.38, $CHCl_3$). IR (neat, cm^{-1}): 3272 (br), 2861 (w), 1713 (m), 1668 (s), 1476 (m), 1342 (w). ^1H NMR (500 MHz, $CDCl_3$): δ 9.76 (s, 1H), 8.03 (d, $J = 7.7$ Hz, 1H), 7.44 (dt, $J = 1.4$, 7.5 Hz, 1H), 7.35 (t, $J = 7.6$ Hz, 1H), 7.30 (br s, 1H), 7.21 (d, $J = 7.5$ Hz, 1H), 3.74 (dd, $J = 4.2$, 12.6 Hz, 1H), 3.60−3.54 (m, 1H), 3.42−3.38 (m, 1H), 2.98 (dd, $J = 8.3$, 18.3 Hz, 1H), 2.73 (dd, $J = 5.3$, 18.3 Hz, 1H). ^{13}C NMR (125 MHz, $CDCl_3$): δ 199.9, 166.3, 141.4, 132.6, 128.3, 128.2, 127.6, 126.8, 47.0, 44.0, 31.7. LRMS (ES^+): 212 (M + Na). HRMS (ES^+): *m/z* 212.0695 [$(M + Na)^+$; calcd for $C_{11}H_{11}NO_2Na$, 212.0687; $\sigma = -3.6$ ppm].

Monopyrrolinone (+)-34. The aldehyde (+)-**25** (32 mg, 0.169 mmol) and amino ester (+)-**8**[14b] (79 mg, 0.164 mmol) were dissolved in toluene (6 mL) and concentrated in vacuo with mild heating; this process was repeated 10 times, and the residue was placed under vacuum for 1 h. The flask was then placed under argon and charged with THF (11 mL), and KHMDS (1.49 mL of a 0.5 M solution in toluene, 0.745 mmol) was added; the solution turned green immediately and then after a few minutes turned orange. After 20 min, a 10% aqueous solution of $KHSO_4$ (10 mL) was added, the aqueous phase was extracted with EtOAc (3 × 50 mL), and the combined organic phases were dried ($MgSO_4$), filtered, and concentrated in vacuo. Flash chromatography (9:1 EtOAc/MeOH) followed by preparative TLC (95:5 CH_2Cl_2/MeOH) furnished (+)-**34** (52 mg, 51%) as a light yellow solid: mp 234−236 °C (CH_2Cl_2/pentane); $[\alpha]_D$ + 84.9 (*c* 1.33, $CHCl_3$). IR (neat, cm^{-1}): 3241 (br), 2968 (w), 2922 (w), 2359 (m), 1697 (s), 1674 (s), 1653 (s), 1558 (s), 1393 (s), 1365 (m), 1176 (m). ^1H NMR [mixture of rotamers] (500 MHz, $CDCl_3$): δ 7.99−7.97 (m, 1H), 7.34−7.21 (m, 9H), 7.16 (d, $J = 6.3$ Hz, 1H), 7.05 (d, $J = 6.3$ Hz, 1H), 6.85 (br s, 1H), 6.83−6.81 (m, 1H), 5.18 (br s, 0.4H), 5.11 (br s, 1H), 5.05 (br s, 0.6H), 3.83 (br s, 1H), 3.65 (br s, 2H), 3.42 (dd, $J = 3.7$, 12.2 Hz, 1H), 3.26 (br s, 0.6H), 3.05 (br s, 0.4H), 3.00−2.86 (br m, 3H), 2.76 (d, $J = 13.1$ Hz, 1H), 2.12 (br s, 0.6H), 2.03 (br s, 0.4H), 1.91 (dd, $J = 7.9$, 14.5 Hz, 1H), 1.52 (s, 9H), 1.51−1.41 (br s, 3H), 0.92 (br s, 1H), 0.77 (br s, 2H). ^{13}C NMR (125 MHz, $CDCl_3$): δ 201.2, 165.3, 162.8, 140.3, 137.0, 135.0, 132.4, 130.5, 130.3, 128.5, 128.3, 128.0, 127.8, 127.3, 127.0, 126.7, 126.7, 114.3, 80.1, 77.0, 70.1, 63.3, 43.6, 43.0, 42.9, 32.3, 28.5, 25.7. LRMS (ES^+): 1265 (2M + Na), 644 (M + Na). HRMS (ES^+): *m/z* 644.3134 [$(M + Na)^+$; calcd for $C_{38}H_{43}N_3O_5Na$, 644.3100; $\sigma = -5.2$ ppm].

Tetrahydroisoquinolyl Inhibitor (+)-24. To a solution of (+)-**34** (36 mg, 0.058 mmol) in CH_2Cl_2 (2 mL) at 0 °C was added trifluoroacetic acid (5 mL), and after 1 h, water was added (5 mL), and the solution was stirred at room temperature for 72 h. Upon completion, as monitored by LRMS, toluene (50 mL) was added and the solvent was concentrated in vacuo to one-half volume. This process was repeated three times, before completely concentrating the solution. The resulting solid was dissolved in MeOH and filtered, and the filtrate was concentrated in vacuo. The residue was placed under vacuum for 2 h and dissolved in CH_2Cl_2 (15 mL), and Et_3N (0.057 mL, 0.406 mmol) was added, followed after 5 min by (+)-**20** (16 mg, 0.070 mmol). After 3 h, saturated NH_4Cl (6 mL) was added, the aqueous phase was extracted with CH_2Cl_2 (4 × 20 mL), and the combined organic phases were dried (Na_2SO_4), filtered, and concentrated in vacuo. Flash chromatography (98:2 EtOAc/MeOH) afforded (+)-**24** as a beige crystalline solid (26 mg, 76%). Before submission for biological testing, (+)-**24** was repurified by recrystallization (CH_2Cl_2/pentane) or by preparative RP-HPLC [column, C18 Dynamax 300 Å (21.4 mm × 250 mm); isocratic 65% water−35% MeCN; flow rate, 10 mL/min] to give >98% purity by HPLC in two different systems: mp 228−230 °C; $[\alpha]_D$ + 55 (*c* 0.06, $CHCl_3$). IR (neat): 3275 (br), 2927 (w), 2874 (w), 1704 (m), 1657 (s), 1551 (m), 1494 (w), 1454 (w) 1337 (w), 1276 (w), 1172 (w), 1080 (w), 1033 (w) cm^{-1}. ^1H NMR (500 MHz, $CDCl_3$, 304 K) mixture of rotamers: δ 8.01 (dd, $J = 1.0$, 7.7 Hz, 1H), 7.44 (t, $J = 7.3$ Hz, 1H), 7.37−7.34 (m, 1H), 7.33−7.27 (m, 4H), 7.24−7.20 (m, 3H), 7.18−7.15 (m, 0.2H), 7.12 (d, $J = 7.5$ Hz, 0.8H), 7.01 (d, $J = 4.0$ Hz, 1H), 6.98−6.95 (m, 0.4H), 6.93 (d, $J = 7.3$ Hz, 1.6H), 5.61 (br s, 0.2H), 5.51 (br d, $J = 3.4$ Hz, 0.8H), 5.16 (d, $J = 9.3$ Hz, 1H), 5.15−5.13 (m, 1H), 5.08−5.06 (m, 0.8H), 5.03−4.98 (m, 0.2H), 4.99 (br s, 0.2H), 4.76 (br s, 0.8H), 4.10−4.04 (m, 0.2H), 4.02 (d, $J = 9.4$ Hz, 0.8H), 3.90−3.86 (m, 2H), 3.82−3.77 (m, 2H), 3.71 (d, $J = 9.9$ Hz, 1H), 3.64 (q, $J = 8.1$ Hz, 1H), 3.62−3.58 (m, 0.4H), 3.51−3.49 (m, 1.6H), 3.10−3.01 (m,

1H), 2.97−2.88 (m, 2H), 2.92 (AB quartet, J = 13.2 Hz, 2H), 2.14−2.06 (m, 1H), 1.97−1.93 (m, 1H), 1.82 (dd, J = 10.2, 14.3 Hz, 1H), 1.70 (d, J = 13.9 Hz, 1H). ^{1}H NMR (500 MHz, $CDCl_3$, 320 K): 8.07 (dd, J = 1.3, 7.7 Hz, 1H), 7.48 (dt, J = 1.3, 7.4 Hz, 1H), 7.40 (dt, J = 1.3, 7.6 Hz, 1H), 7.38−7.35 (m, 1H), 7.32−7.30 (m, 4H), 7.28−7.24 (m, 3H), 7.15 (d, J = 7.2 Hz, 1H), 7.08 (d, J = 3.9 Hz, 1H), 7.00 (d, J = 7.1 Hz, 2H), 5.45 (br s, 1H), 5.18−5.12 (br m, 3H), 4.51 (br s, 1H), 4.04 (br d, J = 7.9 Hz, 1H), 3.91 (br s, 2H), 3.89−3.82 (br m, 2H), 3.75 (d, J = 10.3 Hz, 1H), 3.73−3.67 (br m, 1H), 3.54 (dd, J = 3.3, 12.1 Hz, 1H), 3.16−3.08 (m, 1H), 3.06 (d, J = 13.4 Hz, 1H), 3.01−2.94 (m, 1H), 2.96 (AB quartet, J = 13.5 Hz, 2H), 2.17−2.11 (br m, 1H), 2.09−1.99 (br m, 1H), 1.86 (dd, J = 10.0, 14.3 Hz, 1H), 1.78 (br d, J = 13.5 Hz, 1H). ^{13}C NMR (125 MHz, $CDCl_3$, 304 K): δ 203.2, 165.5, 162.5, 156.3, 140.2, 138.1, 134.6, 130.2, 129.3, 128.5, 128.3, 128.0, 127.5, 127.0, 126.5, 112.4, 75.3, 73.3, 70.5, 67.4, 66.9, 58.6, 57.7, 43.6, 41.6, 39.8, 39.5, 38.9, 32.7, 32.2, 29.6. COSY; HMQC; LRMS (ES^+): 1213 (2M + Na), 618 (M + Na). HRMS (ES^+): m/z 618.2606 [$(M + Na)^+$; calcd for $C_{35}H_{37}N_3O_6Na$, 618.2580; σ = −4.3 ppm]; X-ray.

Acknowledgment. We are pleased to acknowledge support of this investigation by the National Institutes of Health through Grant GM-41821 (Institute of General Medical Sciences) and Grant AI-42010 (Institute of Allergy and Infectious Diseases). Additional funding was provided by Bachem Inc. (Torrence, CA), Merck Research Laboratories (West Point, PA), and Saynkyo Co., Ltd. (Tokyo, Japan). We thank Dr. G. Furst, Dr. P. Carroll, Mr. J. Dykins, and Dr. R. Kohli, Directors of the University of Pennsylvania Spectroscopic Facilities, for assistance in obtaining NMR spectra, small-molecule X-ray crystal structures, and high-resolution mass spectra, respectively. We also thank Dr. Donald Heefner, Dr. Joel Huff (Merck Research Laboratories, West Point), Mr. Charles A. Lesburg, and Dr. Christopher S. Shiner for helpful suggestions and critical comments.

Supporting Information Available: X-ray crystallographic data for (+)-**24**. This material is available free of charge via the Internet at http://pubs.acs.org.

References

(1) (a) Ratner, L.; Haseltine, W.; Patarca, R.; Livak, K. J.; Starcich, B.; Joseph, S. F.; Doran, E. R.; Rafalski, J. A.; Whitehorn, E. A.; Baumeister, K.; Ivanoff, L.; Petteway, S. R., Jr.; Pearson, M. L.; Lautenberger, J. S.; Papas, T. K.; Ghrayeb, J.; Chang, N. T.; Gallo, R. C.; Wong-Staal, F. Complete Nucleotide Sequence of the AIDS Virus, HTLV−III. *Nature* **1985**, *313*, 277−284. (b) Hu, Y.-W.; Kang, C. Y. Enzyme Activities in Four Different Forms of Human Immunodeficiency Virus 1 *pol* Gene Products. *Proc. Natl. Acad. Sci. U.S.A.* **1991**, *88*, 4596−4600. (c) Sayasith, K.; Sauve, G.; Yelle, J. Targeting HIV-1 Integrase. *Exp. Opin. Ther. Targets* **2001**, *5*, 443−464.

(2) Ruprecht, R. M.; O'Brien, L. G.; Rossoni, L. D.; Nusinoff-Lehrman, S. Suppression of Mouse Viraemia and Retroviral Disease by 3′-azido-3′-deoxythymidine. *Nature* **1986**, *323* (6087), 467−469.

(3) (a) Bursavich, M. G.; Rich, D. H. Designing Non-Peptide Peptidomimetics in the 21st Century: Inhibitors Targeting Conformational Ensembles. *J. Med. Chem.* **2002**, *45*, 541−558. (b) Brik, A.; Wong, C.-H. HIV-1 Protease: Mechanism and Drug Discovery. *Org. Biomol. Chem.* **2003**, *1*, 5−14.

(4) (a) Molla, A.; Granneman, G. R.; Sun, E.; Kempf, D. J. Recent Developments in HIV Protease Inhibitor Therapy. *Antiviral Res.* **1998**, *39*, 1−23. (b) Kemptf, D. J.; Sham, H. L. HIV Protease Inhibitors. *Curr. Pharm. Des.* **1996**, *2*, 225−246. (c) Garg, R.; Gupta, S. P.; Gao, H.; Babu, M. S.; Debnath, A. K.; Hansch, C. Comparative Quantitative Structure−Activity Relationship Studies on Anti-HIV Drugs. *Chem. Rev.* **1999**, *99*, 3225−3601.

(5) (a) Boden, D.; Markowiz, M. Resistance to Human Immunodeficiency Virus Type 1 Protease Inhibitors. *Antimicrob. Agents Chemother.* **1998**, *42*, 2775−2783. (b) Tisdale, M.; Myers, R. E.; Maschera, B.; Parry, N.; Oliver, N. M.; Blair, E. D. Cross-Resistance Analysis of Human Immunodeficiency Virus Type 1 Variants Individually Selected for Resistance to Five Different Protease Inhibitors. *Antimicrob. Agents Chemother.* **1995**, *39*, 1704−1710. (c) Jacobsen, H.; Yasargil, K.; Winslow, D. L.; Craig, J. C.; Kroehn, A.; Duncan, I. B.; Mous, J. Characterization of Human Immunodeficiency Virus Type 1 Mutants with Decreased Sensitivity to Proteinase Inhibitor Ro 31−8959. *Virology* **1995**, *206*, 527−534.

(6) (a) Martinez, E.; Mocroft, A.; García-Viejo, M. A.; Pérez-Cuevas, J. B.; Blanco, J. L.; Mallolas, J.; Bianchi, L.; Conget, I.; Blanch, J.; Phillips, A.; Gatell, M. Risk of Lypodystrophy in HIV-1-infected Patients Treated with Protease Inhibitors: A Propective Cohort Study. *Lancet* **2001**, *357*, 592−598. (b) For a recent review, see Dubé, M. P. Disorders of Glucose Metabolism in Patients Infected with Human Immunodeficiency Virus. *Clin. Infect. Dis.* **2000**, *31*, 1467−1475.

(7) (a) Swantstrom, R.; Erona, J. Human Immunodeficiency Virus Type 1 Protease Inhibitors: Therapeutic Successes and Failures, Supression and Resistance. *Pharmacol. Ther.* **2000**, *86*, 145−170. (b) Carpenter, C.; Cooper, D. A.; Fischl, M. Antiretroviral Therapy in Adults: Updated Recommendations of the International AIDS Society-USA Panel. *JAMA, J. Am. Med. Assoc.* **2000**, *283*, 381−390. (c) Centers for Disease Control and Prevention. Guidelines for the Use of Antiretroviral Therapy in HIV−Infected Adults and Adolescents. *MMWR Morb. Mortal. Wkly. Rep.* **1998**, *49* (RR-5), 43−82. (d) De Clercq, E. Perspectives of Non-Nucleoside Reverse Transcriptase Inhibitors (NNRTIs) in the Therapy of HIV-1 Infection. *Farmaco* **1999**, *54*, 26−54. (e) De Clercq, E. Recent Developments in the Chemotherapy of HIV Infections. *Pure Appl. Chem.* **1998**, *70*, 567−577.

(8) (a) Thaisrivongs, S.; Tomich, P. K.; Watenpaugh, K. D.; Chong, K.-T.; Howe, W. J.; Yang, C.-P.; Strohbach, J. W.; Turner, S. R.; McGrath, J. P.; Bohanon, M. J.; Lynn, J. C.; Mulichak, A. M.; Spinelli, P. A.; Hinshaw, R. R.; Pagano, P. J.; Moon, J. B.; Ruwart, M. J.; Wilkinson, K. F.; Rush, B. D.; Zipp, G. L.; Dalga, R. J.; Schwende, F. J.; Howard, G. M.; Padbury, G. E.; Toth, L. N.; Zhao, Z.; Koeplinger, K. A.; Kakuk, T. J.; Cole, S. L.; Zaya, R. M.; Piper, R. C.; Jeffrey, P. Structure-Based Design on HIV Protease Inhibitors: 4-Hydroxycoumarins and 4-Hydroxy-2-pyrones as Non-Peptidic Inhibitors. *J. Med. Chem.* **1994**, *37*, 3200−3204. (b) Turner, S. R.; Strohbach, J. W.; Tommasi, R. A.; Aristoff, P. A.; Johnson, P. D.; Skulnick, H. I.; Dolak, L. A.; Seest, E. P.; Tomich, P. K.; Bohanon, M. J.; Horng, M.-M.; Lynn, J. C.; Chong, K.-T.; Hinshaw, R. R.; Watenpaugh, K. D.; Janakiramam, M. N.; Thaisrivongs, S. Tipranavir (PNU-140690): A Potent, Orally Bioavailable Nonpeptidic HIV Protease Inhibitor of the 5,6-Dihydro-4-hydroxy-2-pyrone Sulfonamide Class. *J. Med. Chem.* **1998**, *41*, 3467−3476.

(9) Lam, P. Y. S.; Jadhav, P. K.; Eyermann, C. J.; Hodge, C. N.; Ru, Y.; Bacheler, L. T.; Meek, O. M. J.; Rayner, M. M. Rational Design of Potent, Bioavailable, Nonpeptide Cyclic Ureas as HIV Protease Inhibitors. *Science* **1994**, *263*, 380−384.

(10) (a) Smith, A. B., III; Keenan, T. P.; Holcomb, R. C.; Sprengeler, P. A.; Guzman, M. C.; Wood, J. L.; Carroll, P. J.; Hirschmann, R. Design, Synthesis, and Crystal Structure of a Pyrrolinone-Based Peptidomimetic Possessing the Conformation of a β-Strand: Potential Application to the Design of Novel Inhibitors of Proteolytic Enzymes. *J. Am. Chem. Soc.* **1992**, *114*, 10672−10674. (b) Smith, A. B., III; Guzman, M. C.; Sprengeler, P. A.; Keenan, T. P.; Holcomb, R. C.; Wood, J. L.; Carroll, P. J.; Hirschmann, R. De Novo Design, Synthesis, and X-ray Crystal Structures of Pyrrolinone-Based β−Strand Peptidomimetics. *J. Am. Chem. Soc.* **1994**, *116*, 9947−9962.

(11) Leung, D.; Abbenante, G.; Fairlie, D. P. Protease Inhibitors: Current Status and Future Prospects. *J. Med. Chem.* **2000**, *3*, 305−340.

(12) Smith, A. B., III; Wang, W.; Sprengeler, P. A.; Hirschmann, R. Design, Synthesis, and Solution Structure of a Pyrrolinone-Based β-Turn Peptidomimetic. *J. Am. Chem. Soc.* **2000**, *122*, 11037−11038.

(13) (a) Smith, A. B., III; Akaishi, R.; Jones, D. R.; Keenan, T. P.; Guzman, M. C.; Holcomb, R. C.; Sprengeler, P. A.; Wood, J. L.; Hirschmann, R.; Holloway, M. K. Design and Synthesis of Non-Peptide Peptidomimetic Renin Inhibitors. *Biopolymers (Peptide Sci.)* **1995**, *37*, 29−53. (b) Smith, A. B., III; Hirschmann, R.; Pasternak, A.; Akaishi, R.; Guzman, M. C.; Jones, D. R.; Keenan, T. P.; Sprengeler, P. A.; Darke, P. L.; Emini, E. A.; Holloway, M. K.; Schleif, W. A. Design and Synthesis of Peptidomimetic Inhibitors of HIV-1 Protease and Renin. Evidence for Improved Transport. *J. Med. Chem.* **1994**, *37*, 215−218.

(14) (a) Smith, A. B., III; Hirschmann, R.; Pasternak, A.; Yao, W.; Sprengeler, P. A.; Holloway, M. K.; Kuo, L. C.; Chen, Z.; Darke, P. L.; Schleif, W. A. An Orally Bioavailable Pyrrolinone Inhibitor of HIV-1 Protease: Computational Analysis and X-ray Crystal Structure of the Enzyme Complex. *J. Med. Chem.* **1997**, *40*, 2440−2444. (b) Smith, A. B., III; Hirschmann, R.; Pasternak, A.; Guzman, M. C.; Yokoyama, A.; Sprengeler, P. A.; Darke, P. L.; Emini, E. A.; Schleif, W. A. Pyrrolinone-Based HIV Protease Inhibitors. Design, Synthesis and Antiviral Activity: Evidence for Improved Transport. *J. Am. Chem. Soc.* **1995**, *117*, 11113−11123.

(15) Smith, A. B., III; Nittoli, T.; Sprengeler, P. A.; Duan, J. J.-W.; Liu, R.-Q.; Hirschmann, R. F. Design, Synthesis, and Evaluation of a Pyrrolinone-Based Matrix Metalloprotease Inhibitor. *Org. Lett.* **2000**, *2*, 3809−3812.

(16) (a) Smith, A. B., III; Benowitz, A. B.; Guzman, M. C.; Sprengeler, P. A.; Hirschmann, R.; Schweiger, E. J.; Bolin, D. R.; Nagy, Z.; Campbell, R. M.; Cox, D. C.; Olson, G. L. Design, Synthesis, and Evaluation of a Pyrrolinone-Peptide Hybrid Ligand for the Class II MHC Protein HLA-DR1. *J. Am. Chem. Soc.* **1998**, *120*, 12704−12705. (b) Smith, A. B., III; Benowitz, A. B.; Sprengeler, P. A.; Barbosa, J.; Guzman, M. C.; Hirschmann, R.; Schweiger, E. J.; Bolin, D. R.; Nagy, Z.; Campbell, R. M.; Cox, D. C.; Olson, G. L. Design and Synthesis of a Competent Pyrrolinone-Peptide Hybrid Ligand for the Class II Major Histocompatibility Complex Protein HLA-DR1. *J. Am. Chem. Soc.* **1999**, *121*, 9286−9298.

(17) (a) We employ C/I ratios rather than I/C ratios to quantify transport because the former values are usually >1 and the latter <1; cf., Thompson, W. J.; Fitzgerald, P. M. D.; Holloway, M. K.; Emini, E. A.; Darke, P. L.; McKeever, B. M.; Schleif, W. A.; Quintero, J. C.; Zugay, J. A.; Tucker, T. J.; Schwering, J. E.; Homnick, C. F.; Nunberg, J.; Springer, J. P.; Huff, J. R. Synthesis and Antiviral Activity of a Series of HIV-1 Protease Inhibitors with Functionality Tethered to the P1 or P1′ Phenyl Substituents: X-ray Crystal Structure Assisted Design. *J. Med. Chem.* **1992**, *35*, 1685−1701. (b) For an application of the I/C ratio, see Smith, R. A.; Coles, P. J.; Chen, J. J.; Robinson, V. J.; MacDonald, I. D.; Carriere, J.; Krantz, A. Design, Synthesis, and Activity of Conformationally-Constrained Macrocyclic Peptide-Based Inhibitors of HIV Protease. *Bioorg. Med. Chem. Lett.* **1994**, *4*, 2217−2222.

(18) (a) Smith, A. B., III; Hirschmann, R.; Pasternak, A.; Akaishi, M.; Guzman, M. C.; Jones, D. R.; Keenan, T. P.; Sprengeler, P. A.; Darke, P. L.; Emini, E. A.; Holloway, M. K.; Schleif, W. A. Design and Synthesis of Peptidomimetic Inhibitors of HIV-1 Protease and Renin. Evidence for Improved Transport. *J. Med. Chem.* **1994**, *37*, 215−218. (b) Smith, A. B., III; Hirschmann, R.; Pasternak, A.; Guzman, M. C.; Sprengeler, P. A. Pyrrolinone Based HIV Protease Inhibitors. Design, Synthesis, and Antiviral Activity; Evidence for Improved Transport. *J. Am. Chem. Soc.* **1995**, *117*, 11113−11123.

(19) (a) Lyle, T. A.; Wiscount, C. M.; Guare, J. P.; Thompson, W. J.; Anderson, P. S.; Darke, P. L.; Zugay, J. A.; Emini, E. A.; Schleif, W. A.; Quintero, J. C.; Dixon, R. A. F.; Sigal, I. S.; Huff, J. R. Benzocycloalkylamines as Novel C-Termini for HIV Protease Inhibitors. *J. Med. Chem.* **1991**, *34*, 1228−1230. (b) Ghosh, A. K.; Thompson, W. J.; McKee, S. P.; Duong, T. T.; Lyle, T. A.; Chen, J. C.; Darke, P. L.; Zugay, J. A.; Emini, E. A.; Schleif, W. A.; Huff, J. R.; Anderson, P. S. 3-Tetrahydrofuran and Pyran Urethanes as High-Affinity P2-Ligands for HIV-1 Protease Inhibitors. *J. Med. Chem.* **1993**, *36*, 292−294.

(20) (a) Miller, M.; Schneider, J.; Sathyanarayana, B. K.; Toth, M. V.; Marshall, G. R.; Clawson, L.; Selk, L. M.; Kent, S. B. H.; Wlodawer, A. Structure of Complex of Synthetic HIV-1 Protease with a Substrate-Based Inhibitor at 2.3 Å Resolution. *Science* **1989**, *246*, 1149−1152. (b) Swain, A. L.; Miller, M. M.; Green, J.; Rich, D. H.; Schneider, J.; Kent, S. B. H.; Wlodawer, A. X-ray Crystallographic Structure of a Complex between a Synthetic Protease of Human Immunodeficiency Virus 1 and a Substrate-Based Hydroxyethylamine Inhibitor. *Proc. Natl. Acad. Sci. U.S.A.* **1990**, *87*, 8805−8809.

(21) Holloway, M. K.; Wai, J. M.; Halgren, T. A.; Fitzgerald, P. M. D.; Vacca, J. P.; Dorsey, B. D.; Levin, R. B.; Thompson, W. J.; Chen, L. J.; deSolms, S. J.; Gaffin, N.; Ghosh, A. K.; Giuliani, E. A.; Graham, S. L.; Guare, J. P.; Hungate, R. W.; Lyle, T. A.; Sanders, W. M.; Tucker, T. J.; Wiggins, M.; Wiscount, C. M.; Woltersdorf, O. W.; Young, S. D.; Darke, P. L.; Zugay, J. A. A Priori Prediction of Activity for HIV-1 Protease Inhibitors Employing Energy Minimization in the Active Site. *J. Med. Chem.* **1995**, *38*, 305−317.

(22) Smith, A. B., III; Akaishi, M.; Guzman, M. C.; Holcomb, R. C.; Jones, D. R.; Keenan, T. P.; Sprengeler, P. A.; Wood, J. L.; Hirschmann, R.; Holloway, M. K. Design and Synthesis of Non-peptide Peptidomimetic Inhibitors of Renin. *Biopolymers (Peptide Sci.)* **1995**, *37*, 29−53.

(23) (a) Cyclobutanone **10** was prepared from indene via a modification of a published sequence: Jeffs, P. W.; Molina, G.; Cass, M. W.; Cortese, N. A. Synthesis of 1-Substituted *cis*-Bicyclo[4.2.0]-octanones through [2 + 2] Cyclcoadditions of Dichloroketene to Alkenes. Structural Characterization of Cycloadducts by Oxa-Ring Expansion. *J. Org. Chem.* **1982**, *47*, 3871−3875. (b) Dechlorination: Pak, C. S.; Kim, S. K. A Convenient Regioselective Synthesis of Substituted Cycloheptenones. *J. Org. Chem.* **1990**, *55*, 1954−1957.

(24) (a) Johnson, C. R.; Zeller, J. R. Sulfoximine-Mediated Resolutions of Ketones. *J. Am. Chem. Soc.* **1982**, *104*, 4021−4023. (b) Johnson, C. R.; Zeller, J. R. *N*,*S*-Dimethyl-*S*-Phenylsulfoximine—A Reagent for the Optical Resolution of Ketones. *Tetrahedron* **1984**, *40*, 1225−1233.

(25) Corey, E. J.; Arnold, Z.; Hutton, J. Total Synthesis of Prostaglandins E2 and F2 (dl) via a Tricarbocyclic Intermediate. *Tetrahedron Lett.* **1970**, *4*, 307−310.

(26) Basha, A.; Lipton, M.; Weinreb, S. M. A Mild, General Method for Conversion of Esters to Amides. *Tetrahedron Lett.* **1977**, *48*, 4171−4174.

(27) Thompson, W. J.; Vacca, J. P.; Huff, J. R.; Lyle, T. A.; Young, S. D.; Hungate, R. W.; Britcher, S. F.; Ghosh, A. K. European Patent Application EP 434365, 1991.

(28) Olsen, D. B.; Stahlhut, M.; Rutkowski, C.; Schock, H. B.; vanOlden, A. L.; Kuo, L. C. Non-Active Site Changes Elicit Broad-Based Cross-Resistance of the HIV-1 Protease to Inhibitors. *J. Biol. Chem.* **1999**, *274*, 23699−23701.

(29) For information on the cellular assays and oral bioavailability studies, see Vacca, J. P.; Dorsey, B. D.; Schleif, W. A.; Levin, R. B.; McDaniel, S. L.; Darke, P. L.; Zugay, J.; Quintero, J. C.; Blahy, O. M.; Roth, E.; Sardana, V. V.; Schlabach, A. J.; Grahm, P. I.; Condra, J. H.; Gotlib, L.; Holloway, M. K.; Lin, J.; Chen, I.-W.; Vastag, K.; Ostovic, D.; Anderson, P. S.; Emini, E. A.; Huff, J. R. L-735-524—An Orally Bioavailable Human-Immunodeficiency-Virus Type-1 Protease Inhibitor. *Proc. Natl. Acad. Sci. U.S.A.* **1994**, *91*, 4096−4100.

(30) Single crystals, obtained at room temperature via vapor diffusion in hanging drops diffracted to 2.0 Å resolution. The space group was $P2_12_12$ (cell constants: $a = 58.26$ Å, $b = 87.48$ Å, and $c = 46.41$ Å) with one molecule of the complex per asymmetric unit. Following data collection and processing, as described previously, the structure was determined via the difference Fourier method, using the Indinavir complex as the starting model. The structure was refined with XPLOR using data between 2 and 6 Å resolution yielding an *R* factor of 0.183 with rms bond length and bond angle deviations of 0.016 Å and 2.048°, respectively. A single orientation was observed for (−)-**7** bound to the protease. This structure has been deposited with the Protein Data Bank with access number 1NPA.

(31) Figures 4−7 were prepared using the Insight II software (Molecular Simulations Inc., San Diego, CA).

(32) Chen, Z.; Li, Y.; Chen, E.; Hall, D.; Darke, P. L.; Shafer, J. A.; Kuo, L. C. Crystal Structure at 1.9 Å Resolution of HIV-2 Protease Complexed with L-735,524: An Orally Bioavailable Inhibitor of the HIV Proteases. *J. Biol. Chem.* **1994**, *269*, 26344−26348.

(33) Despite similar side chain positioning by two nonpeptide inhibitors, one inhibitor was observed to interact with the enzyme Asp30 via a water molecule, whereas the other inhibitor interacts directly with Asp30. Romines, K. R.; Watenpaugh, K. D.; Howe, W. J.; Tomich, P. K.; Lovasz, K. D.; Morris, J. K.; Janakiraman, M. N.; Lynn, J. C.; Horng, M.-M.; Chong, K.-T.; Hinshaw, R. R.; Dolak, L. A. Structure-Based Design of Nonpeptide HIV Protease Inhibitors from a Cyclooctylpyranone Lead Stucture. *J. Med. Chem.* **1995**, *38*, 4463−4473.

(34) (a) Klebe, G.; Bohm, H.-J. Energetic and Entropic Factors Determining Binding Affinity in Protein−Ligand Complexes. *J. Recept. Signal Transduction Res.* **1997**, *17* (1−3), 459−473. (b) Murcko, A.; Murcko, M. A. Computational Methods to Predict Binding Free Energy in Ligand−Receptor Complexes. *J. Med. Chem.* **1995**, *26*, 4953−4963.

(35) (a) Jordan, D. B.; Basarab, G. S. Binding Dynamics of Two Water Molecules Constrained within the Scytalone Dehydratase Binding Pocket. *Bioorg. Med. Chem. Lett.* **2000**, *10*, 23−26. (b) Chen, J. M.; Xu, S. L.; Wawrzak, Z.; Basarab, G. S.; Jordan, D. B. Structure-Based Design of Potent Inhibitors of Scytalone Dehydratase: Displacement of a Water Molecule from the Active Site. *Biochemistry* **1998**, *37*, 17735−17744. (c) Prasad, J. V. N. V.; Lunney, E. A.; Ferguson, D.; Tummino, P. J.; Rubin, J. R.; Reyner, E. L.; Stewart, B. H.; Guttendorf, R. J.; Domagala, J. M.; Suvorov, L. I.; Gulnik, S. V.; Topol, I. A.; Bhat, T. N.; Erickson, J. W. HIV Protease Inhibitors Possessing Novel, High-Affinity, and Achiral P1′/P2′ Ligand with a Unique Pattern of in Vitro Resistance. The Importance of Conformationally-Restricted Template in the Design of Enzyme Inhibitors. *J. Am. Chem. Soc.* **1995**, *117*, 11070−11074. (d) Watson, K. A.; Mitchell, E. P.; Johnson, L. N.; Son, J. C.; Bichard, C. J. F.; Orchard, M. G.; Fleet, G. W. J.; Oikonomakos, N. G.; Leonidas, D. D.; Kontou, M.; Papageorgioui, A. Design of Inhibitors of Glycogen-Phosphorylase—A Study of α-C-Glucosides and β-C-Glucosides and 1-Thio-β-D-Glucose Compounds. *Biochemistry* **1994**, *33*, 5745−5748.

(36) Ladbury, J. E. Just Add Water! The Effect of Water on the Specificity of Protein−Ligand Binding Sites and its Potential Application to Drug Design. *Chem. Biol.* **1996**, *3*, 973−980.

(37) Campiani, G.; Kozikowski, A. P.; Wang, S.; Ming, L.; Nacci, V.; Sazena, A.; Doctor, B. P. Synthesis and Anticholinesterase Activity of Huperzine A Analogues Containing Phenol and Cathechol Replacements for the Pyridone Ring. *Bioorg. Med. Chem. Lett.* **1998**, *8*, 1413−1418.

(38) Kocovky, P. Carbamates: A Method of Synthesis and Some Synthetic Applications. *Tetrahedron Lett.* **1986**, *27*, 5521−5524.

(39) Single crystals of the (−)-**23**−HIV-1 protease complex diffracted to 2.0 Å resolution. The space group was $P2_12_12$ with crystal unit cell constants $a = 58.26$ Å, $b = 87.46$ Å, and $c = 46.41$ Å. The structure was refined with XPLOR using data between 2 and 6 Å resolution yielding a final *R* factor of 0.188. This structure has been deposited with the Protein Data Bank with access number 1NPW.

(40) (a) Effenberger, F.; Gleiter, R. Friedel−Crafts Reaction of Isocyanates with Benzene Derivatives. *Chem. Ber.* **1964**, *97*, 472−479. (b) Tsuda, Y.; Isobe, K.; Toda, J.; Taga, J. A New Modification of the Bischler-Napieralski Reaction for *β*-arylethyl Isocyanates and *β*-Arylethylurethans. *Heterocycles* **1976**, *5*, 157−162. (c) Schultz, A. G.; Macielag, M.; Podhorez, D. E.; Suhadolnik, J. C.; Kullnig, R. K. Enantioselective Birch Reduction and Reductive Alkylations of Chiral 2-Phenylbenzoic Acid Derivatives. Applicatoin to the Synthesis of Hydrofluoren-9-ones, Hydrophenanthen-9-ones, and (−)-(1*R*,2*R*)-2-Phenylcyclohexanamine. *J. Org. Chem.* **1988**, *53*, 2456−2464. (d) Hanessian, S.; Demont, E.; van Otterlo, W. A. L. From Serine to Functionalized Enantiopure Tetrahydroisoquinolines. *Tetrahedron Lett.* **2000**, *41*, 4999−5003.

(41) Penning, T. D.; Djuric, S. W.; Haack, R. A.; Kalish, V. J.; Miyashiro, J. M.; Rowell, B. W.; Yu, S. S. Improved procedure for the reduction of N-acyloxazolidinones. *Synth. Commun.* **1990**, *20*, 307−312. For preparation, see Tararov, V. I.; Kuznetznov, N. Y.; Bakhmutov, V. I.; Ikonnikov, T. F.; Bubnov, Y. N.; Khrustalev, V. N.; Saveleva, T. F.; Belokon, Y. N. Remarkable Dependence of the Regioselectivity of Free Radical Additions to 3-Cinnamoyloxazolidin-2-ones on the Stability of the Intermediate Adduct-radical, Electrophilicity of the Adding Radicals and the Conditions for their Generation. *J. Chem. Soc., Perkin Trans. 1* **1997**, 3101−3106.

(42) Melnyk, O.; Stephan, E.; Pourcelot, E.; Cresson, P. Additions diastéréosélectives d'alkyl, aryl et allyl cuprates à des imines chirales insaturées. *Tetrahedron* **1992**, *48*, 841−850.

(43) The synthesis of compound (+)-**28** has been reported using different reaction conditions: Wu, M. J.; Wu, C. C.; Lee, P.-C. Lewis acid promoted asymmetric 1,4-addition of allyltrimethylsilanes to chiral α,*β*-unsaturated N-acylamides. *Tetrahedron Lett.* **1992**, *33*, 2547−2548.

(44) Attempts to affect this transformation with the *N*-Boc-protected lactam did not yield any desired pyrrolinone, possibly due to the competitive cyclization of the metalloimine onto the lactam carbonyl.

(45) Single crystals of the (+)-**24**−HIV-1 protease complex diffracted to 2.0 Å resolution. The space group was $P2_12_12$ with crystal unit cell constants $a = 57.98$ Å, $b = 87.53$ Å, and $c = 46.29$ Å. The structure was refined with XPLOR using data between 2 and 6 Å resolution yielding a final *R* factor of 0.210. This structure has been deposited with the Protein Data Bank with access number 1NPV.

(46) Overlays were done with the Insight II software program (Molecular Simulations Inc.). The RMS values were generated by automatically overlaying all of the protease atoms from one protease−inhibitor complex with the protease atoms from another complex and are as follows: indanol (−)-**7**/Indinavir = 0.738; carbamate (−)-**23**/Indinavir = 0.677; lactam (+)-**24**/Indinavir = 0.934; indanol (−)-**7**/carbamate (−)-**23** = 0.577; indanol (−)-**7**/lactam (+)-**24** = 0.702; carbamate (−)-**23**/lactam (+)-**24** = 0.651. We also calculated RMS values after overlaying only the flap region of the proteases interacting with the P2 side chain (residues 44−56) where the most significant changes were observed. The RMS values are as follows: indanol (−)-**7**/Indinavir = 0.834; carbamate (−)-**23**/Indinavir = 0.746; lactam (+)-**24**/Indinavir = 2.912; indanol (−)-**7**/carbamate (−)-**23** = 0.454; indanol (−)-**7**/lactam (+)-**24** = 2.916; carbamate (−)-**23**/lactam (+)-**24** = 2.867.

(47) Heefner, D. L. Unpublished results, Sepracor Inc., Marlborough, MA.

JM0204587